Constraints on the timing of debris-covered and rock glaciers: An exploratory case study in the Hólar area, northern Iceland

José M Fernández-Fernández, David Palacios, Nuria Andrés, Irene Schimmelpfennig, Luis M Tanarro, Skafti Brynjólfsson, Francisco J López-Acevedo, Þorsteinn Sæmundsson

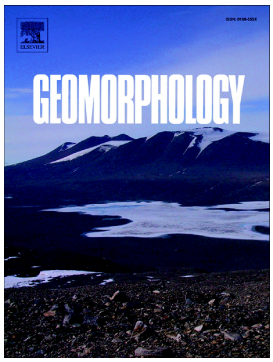

Constraints on the timing of debris-covered and rock glaciers: An exploratory case study in the Hólar area, northern Iceland

José M. Fernández-Fernández, David Palacios, Nuria Andrés, Irene Schimmelpfennig, Luis M. Tanarro, Skafti Brynjólfsson, Francisco J. López-Acevedo, Þorsteinn Sæmundsson, A.S.T.E.R. Team

PII: S0169-555X(20)30168-9

DOI: https://doi.org/10.1016/j.geomorph.2020.107196

Reference: GEOMOR 107196

To appear in: *Geomorphology*

Received date: 3 October 2019

Revised date: 15 February 2020

Accepted date: 1 April 2020

Please cite this article as: J.M. Fernández-Fernández, D. Palacios, N. Andrés, et al., Constraints on the timing of debris-covered and rock glaciers: An exploratory case study in the Hólar area, northern Iceland, *Geomorphology* (2020), https://doi.org/10.1016/j.geomorph.2020.107196

Constraints on the timing of debris-covered and rock glaciers: an exploratory case study in the Hólar area, northern Iceland

José M. Fernández-Fernández[(1)], David Palacios[(1)], Nuria Andrés[(1)], Irene Schimmelpfennig[(2)], Luis M. Tanarro[(1)], Skafti Brynjólfsson[(3)], Francisco J. López-Acevedo[(1)], Þorsteinn Sæmundsson[(4)], ASTER Team[(2)]

[(1)] High Mountain Physical Geography Research Group. Department of Geography, Complutense University of Madrid, 28040 Madrid, Spain.

[(2)] Aix-Marseille Université, CNRS, IRD, INRA Coll. France, CEREGE, Technopôle de l'Environnement Arbois-Méditerranée, BP 80, 13545 Aix-en-Provence, France.

[(3)] Icelandic Institute of Natural History, Borgum vid Norðurslóð, Box 180, 602 Akureyri, Iceland.

[(4)] Faculty of Life and Environmental Science, University of Iceland, Askja, Sturlugata 7, 101 Reykjavík, Iceland.

Abstract

Eighteen samples for ^{36}Cl Cosmic-Ray Exposure (CRE) dating were taken from glacially polished bedrocks, moraine boulders, fossil/active rock glaciers and debris-covered glaciers in Fremri-Grjótárdalur and Hóladalur cirques in the Víðinesdalur, Hofsdalur and Héðinsdalur valleys, close to Hólar village, in the Tröllaskagi peninsula, northern Iceland. Boulder sampling was preceded by a study of the boulder stability with the twofold aim of: ensuring that the surfaces to be sampled were stable enough for the reliable application of CRE dating, and to better understand the relation between the glacier dynamics and exposition history. The results show that the glaciers which occupy the valleys in Tröllaskagi began their retreat around 16 ka. Later, the glaciers advanced again around 11 ka within the cirques, and small moraines were formed. Thereafter, these small glaciers retreated and evolved into rock glaciers as debris from paraglacial processes accumulated on the glacier surface. The fronts of these rock

glaciers stabilized definitively shortly after their formation and became eventually fossil after the melting of their internal ice. New rock glaciers and debris-covered glaciers formed afterwards, which still have internal ice at present, although their current dynamics are mostly related to subsidence. The stabilization of these rock glaciers and debris-covered glaciers is dated to the period between 7 and 3 ka, although they may have been reactivated during cold neoglacial periods. This research demonstrates the potential interest in applying CRE dating methods to debris-covered glaciers and rock glaciers to determine their origin, evolution and phase of cessation of internal movement until they finally lost their internal ice and became fossil.

Keywords: Iceland; deglaciation; rock glaciers; debris-covered glaciers; ^{36}Cl cosmic-ray exposure dating.

1. Introduction

Rock glaciers and debris-covered glaciers are indicative of important tipping point phases in regional climatic and geomorphological evolution (Winkler and Lambiel, 2018, Anderson et al., 2018a). An appropriate differentiation between them allows the understanding of their origin, the palaeoclimatic implications and the geomorphological processes that led to their formation. In this work we follow the differentiation between debris-covered glaciers and rock glacier features proposed by Janke et al. (2015), which can also be applied to their derived landforms, once the internal ice has disappeared in both cases (Fernández-Fernández et al., 2017a). According to this differentiation, the debris-covered glacier surface is characterized by a rock mantle with variable thickness

but overall increasing towards the toe (Janke et al., 2015). Commonly, it shows the presence of longitudinal ridges, no features derived from viscous flow (Clark et al., 1994) and depressions derived from thermokarst and collapse (Janke et al., 2015). The existence of central and lateral moraines is also common (Clark et al., 1994). On the other hand, rock glaciers commonly include transversal ridges and furrows derived from compressive flow and the overlap of shear planes amongst other processes concerning to the debris supply (Janke et al., 2015). Rock glaciers often show some longitudinal ridges resulting from the inclusion of lateral moraines of the original glacier, and also a steep front whose junction with the gentle rock glacier surface is very sharp (Janke et al., 2015).

The existence and dynamics of rock glaciers may indicate permafrost in the region and a Mean Annual Air Temperature (MAAT) $\leq$ -4ºC at present or in the past if they are relict rock glaciers (e.g. Barsch, 1996). Also, they act as fingerprints of the climatic development (i.e., climate warming or moisture supply decrease, and the subsequent mass balance trend) that led to the transformation from debris-free glaciers to rock glaciers (Johnson, 1980; Giardino and Vitek, 1988; Ackert, 1998; Janke et al., 2015; Anderson et al., 2018a; Kenner, 2018 and others), except rock glaciers which have no relationship with a glacial origin (e.g. Barsch, 1996). In this sense, they are affected by the climatic development during their active period (Humlum, 1998; Berger et al., 2005, Paasche et al., 2007; and others), e.g. when an increase in MAAT can either accelerate (Delaloye et al., 2008; Kellerer-Pirklbauer, 2012; Kellerer-Pirklbauer and Kaufmann, 2012; Kellerer-Pirklbauer et al., 2017; Wirz et al., 2016; Eriksen et al., 2018; Kenner, 2018) or stagnate the rock glacier motion (Emmer et al., 2015; Tanarro et al., 2019). Moreover, rock glaciers also reflect the geomorphological changes of the slopes surrounding the rock glaciers (Humlum, 2000), which can transform these rock glaciers

without any direct relationship with climatic changes (Deline et al., 2015; Anderson and Anderson, 2016). And finally, these formations are also indicative of the amount of water supplied to the rock glaciers (Kenner et al., 2018; Jones et al., 2018).

Existence and development of debris-covered glaciers can also indicate climatic and geomorphological changes, such as their origin in the transformation from a debris-free glacier caused by an increase in ablation, the intensification of the geomorphological processes in the surrounding slopes, or the combination of both factors (Kirkbride, 2000, 2011; Brenning, 2005; Azócar and Brenning, 2010; Mayr and Hagg, 2019). Climate changes can also trigger changes in the dynamics of debris-covered glaciers (Hambrey et al., 2008; Benn et al., 2012; Pelto et al., 2013; Glasser et al., 2016). Nevertheless, these changes may also be due to variations in the debris supply derived from the geomorphological activity on the slopes (Anderson and Anderson, 2016; Anderson et al., 2018a; Mayr and Hagg, 2019). In fact, this dual dependence greatly complicates the interpretation of the changes that debris-covered glaciers undergo (Gibson et al., 2017). In this sense, debris-covered glaciers can evolve to rock glaciers throughout various phases driven by climatic evolution and increased debris supply in their environment (Janke et al., 2015; Monnier and Kinnard, 2015; Andrés et al., 2016, Anderson et al., 2018a; Mayr and Hagg, 2019).

Climatic changes, as well as changes in the geomorphological dynamics of the slopes, can directly influence the dynamics of the debris covered glacier and rock glaciers (Anderson et al., 2018a), even leading to the stop of their flow stop or complete melt of their internal ice and stabilization of their deposits (Potter et al., 1998; Janke et al., 2013; Emmer et al., 2015; Tanarro et al., 2019). However, it is very difficult to determine when this transformation occurred (Barsch, 1996; Haeberli et al., 2006). In the light of the presently ongoing global warming, it is particularly important to know

the trend and evolution of these formations and their relation with climate change, as they have been highlighted as authentic water reservoirs (Rangecroft et al., 2015).

Recent intensified studies focus on monitoring dynamics (e.g. mobility) of rock glaciers and debris-covered glaciers on a very reduced time scale, but with increasingly sophisticated techniques (Benn et al., 2012; Bosson and Lambiel, 2016; Capt et al., 2016; Emmer et al., 2015; Lippl et al., 2018 ; Kenner et al., 2018). In spite of the great potential of long-timescale understanding that the dating of active, static or relict rock glaciers and debris-covered glaciers might allow, it has attracted little attention of researchers in recent years in contrast with debris-free glacial chronology, for example, throughout all of North America, where rock glacier landforms are common (Phillips, 2016; Briner et al., 2017; Leonard et al., 2017; Vázquez-Selem and Lachniet, 2017; Licciardi and Pierce, 2018).

The timing of formation of rock glaciers and debris-covered glaciers is often deduced by extrapolating their current dynamics to the past (Ackert, 1998; and many other subsequent studies), without considering the dynamic and morphological changes that these formations can undergo over time (Tanarro et al., 2019). Regional studies have traditionally framed the relative age of rock glaciers within the context of glacial evolution, with support from lake and moraine soil radiocarbon dating (Benedict, 1973; Ribolini et al., 2007 and others).

The need to apply more reliable dating methods to rock glaciers has been proposed for years (Haeberli et al., 2003). Dating rock glaciers methods include:

(i) Lichenometry, from the measurements of lichen growth, the method most commonly applied to rock glaciers (Benedict, 1973; Konrad and Clark, 1998; Galanin et al., 2014 and others) obtains the stabilization point in time of the boulders, within an age range of the last few hundred years, although its application to rock glaciers presents many

difficulties (Rosenwinkel et al., 2015). In any case, it only provides reliable results when independent fixed control points (e.g. historical evidence) are available.

(ii) Radiocarbon dating of lacustrine sediment overridden by rock glaciers (Paasche et al., 2007) or dendrochronology of tree trunks buried by rock glacier debris (Bachrach et al., 2004), although these circumstances very seldomly exist.

(iii) Schmidt Hammer dating to determine the stabilization age of rock glaciers from the rock weathering. As in the case of lichenometry, require complex complementary information to determine the minimum stabilization age, and especially independent fixed points (e.g. surface exposure ages; Matthews et al., 2013; Scapozza et al., 2014; Winkler and Lambiel, 2018).

(iv) Luminescence dating, a method which also presents serious complications of interpretation when applied to rock glaciers (Fuchs et al., 2013).

Over the last ten years, Cosmic-Ray Exposure (CRE) dating methods using beryllium-10 (^{10}Be), helium-3 (^{3}He) and chlorine-36 (^{36}Cl) have been applied to rock glaciers and debris-covered glaciers, although this approach is far from being routine. ^{10}Be dating has been applied successfully to date stabilization time of rock glaciers in Scotland (Ballantyne et al., 2009), the Alps (Hippolyte et al., 2009) and the Iberian Peninsula (Palacios et al., 2017; Rodriguez-Rodriguez et al., 2017; Andrés et al., 2018a). Correlation between ^{10}Be ages and Schmidt Hammer rebound (R- values) to date rock glaciers was shown by Winkler and Lambiel (2018). ^{10}Be dating has also been applied to date the stabilization of fossil debris-covered glaciers (Fernández-Fernández et al., 2017a) and rock avalanche events on active debris-covered glaciers (Deline et al., 2015). ^{3}He has been applied to study the dynamics of debris-covered glaciers (Mackay and Marchant, 2016). ^{36}Cl dating has been successfully applied to date the stabilization period of several rock glaciers in the Iberian Peninsula (Palacios et al., 2012; 2015a,

2015b; 2016), the Alps (Moran et al., 2016); and the Karçal Mountains in the Lesser Caucasus (Dede et al., 2017).

However, a recent application of the CRE methods has shown that boulders on the surface of rock glaciers and debris-covered glaciers with limited flow may have received cosmic radiation before their definitive motionless (Mackay and Marchant, 2016). In fact, active rock glacier ice can be very old; e.g. radiocarbon dating of plant macrofossil remains in a rock glacier core in the Alps yielded an age of >10 ka (Krainer et al., 2015). ^{10}Be dating of boulders from cold based debris-covered glaciers in Antarctica allowed to deduce that the ice is >1 Ma (Mackay and Marchant, 2016) or even >2 Ma old (Bibby et al., 2016). However, it has also been shown that due to the limited trajectory and erosion of the boulders in a rock glacier, they may retain nuclide inheritance prior to deposition (Çiner et al., 2017).

^{36}Cl dating has been successfully applied to basalts, which is the predominant bedrock in Iceland (Swanson and Caffee 2001; Phillips, 2003; Principato et al., 2006; Licciardi et al., 2006; 2007; 2008; Schimmelpfennig 2009; Schimmelpfennig et al., 2009, 2011) has been employed in northern Iceland to date the deglaciation (Principato et al., 2006; Brynjólfsson et al., 2015, Andrés et al., 2018b).

The Tröllaskagi peninsula, in central north Iceland, hosts a total of 167 rock glaciers, debris-covered glaciers and a few debris-free, mostly north-facing (Sigurðsson and Williams, 2008; Icelandic Meteorological Office, 2018; Fig. 1). They are occupying cirques under similar climatic and geomorphological conditions (Björnsson, 1991; Björnsson and Pálsson, 2008). Two of the cirques in the Víðinesdalur valley (Tröllaskagi peninsula) are occupied by rock glaciers and debris-covered glaciers respectively, namely the Fremri-Grjótárdalur cirque, hosting a large rock glacier complex, and the Hóladalur cirque, hosting a large debris-covered glacier,

Hóladalsjökull. A similar debris-covered glacier exists in the Hofsdalur cirque. These rock glaciers and debris-covered glacier have attracted the attention of researchers to determine their flow dynamics (Wangensteen et al., 2006; Farbrot et al., 2007; Kellerer-Pirklbauer et al., 2007; Lilleøren et al., 2013; Tanarro et al., 2019; Campos et al., 2019), but CRE dating methods have not yet been applied (Fig. 1). A combination of multi-temporal aerial photo imagery, lichenometric procedures and ^{36}Cl dating has recently been applied to study the evolution of two nearby debris-free glaciers during late Holocene (Fernández-Fernández et al., 2019).

Here we will present the results of CRE dating of fossil and active rock glacier and debris-covered glacier deposits, which was preceded by high-accuracy boulder tracking measurements of active rock glaciers and debris-covered glaciers, with the objective to relate the results to the stability degree of the analyzed features. The aim of this work is to (i) test the application of CRE dating to determine the stabilization of rock glaciers and debris-covered glaciers of the Tröllaskagi peninsula; and (ii) investigate their evolution to evaluate the potential for future research contributing to our knowledge of the climatic and glacial evolution in this region.

2. Geographic setting.

The Fremri-Grjótárdalur and Hóladalur cirques in the Víðinesdalur valley, and the Hofsdalur and Héðinsdalur valleys are the focus area of this study and are located in the surroundings of the village of Hólar, on the western side of the Tröllaskagi peninsula. These valleys are tributaries to the main valley of Hjaltadalur, which drains into Skagafjörður (Fig. 1), and host both debris-free, debris-covered and rock glaciers. The summits surrounding these cirques form a flat plateau at around 1200-1330 m a.s.l., hosting flat-bottomed cirques with steep 100-170 m high slopes. These cirque walls are composed of Tertiary basalt bedrock, with semi-horizontal lava flows often separated by

30-50 cm thick argillaceous sedimentary layers (Sæmundsson et al., 1980). These walls might have been unstable, as in the rest of Tröllaskagi, and thus are affected by rock slope failures (Jónsson, 1976; Whalley et al., 1983; Mercier et al., 2013; Cossart et al., 2014; Feuillet et al., 2014; Decaulne et al. 2016; Sæmundsson et al. 2018).

The snouts of the debris-covered and rock glaciers in Tröllaskagi are found at 900-950 m a.s.l., where the MAAT is -1.8 to -2.6 ºC (Kellerer-Pirklbauer et al., 2007) and precipitation around 1500-2000 mm (Crochet et al., 2007). The continuous permafrost limit is located between 850-950 m a.s.l. (Wangensteen et al., 2006; Etzelmüller et al., 2007; Czekirda et al., 2019). The current ELA of the main debris-free glaciers close to the study cirques is 1010-1060 m a.s.l., with the MAAT around -2.3 ºC (Fernández-Fernández et al., 2017b). These glaciers reached their LIA maximum ca. 1865-1900, according to Caseldine (1985) or in the 15th century or earlier according to Fernández-Fernández et al. (2019). During this maximum the ELA was about 950-1010 m a.s.l. and the MAAT 1.7-1.9 ºC lower than at present (Caseldine and Stötter, 1993; Fernández-Fernández et al., 2017b).

3. Previous research on the study area.

CRE dating (Andrés et al., 2018b), combined with previous radiocarbon results (see synthesis in Pétursson et al., 2015), indicates that the glacier outlet of the Skagafjörður fjord (Fig. 1), flowing down from the Icelandic Ice Sheet (IIS), was situated in the outermost sector of the fjord at approximately 17-15 ka. Subsequently, this glacier outlet retreated and occupied the central part between 15-12 ka, and then the innermost part of the fjord around 11 ka. After 11 ka, rapid deglaciation affected the fjord, when the IIS outlet glacier almost reached dimensions similar to the current Hofsjökull ice-cap in central Iceland. Norðdahl (1991a, 1991b) emphasized that most of the Tröllaskagi valleys run N-S, thus facilitating the flow of the IIS outlets, but important

secondary valleys in these mountains were outside these flows. Ingólfsson (1991) and Norðdahl (1991a, 1991b) summarized the studies carried out on the possible glaciation of the Tröllaskagi summits and show how most geomorphologists and palaeobotanists in the early 20th century argued for an ice-free scenario for these summits during the LGM. This hypothesis was supported by simulation models (Hubbard et al., 2006). In fact, ice-free plateaus on the Tröllaskagi summits during the LGM may have served as refugia for flora and fauna (Rundgren and Ingólfsson, 1999).

The first study area of this paper includes the two main cirques in the Víðinesdalur valley: Fremri-Grjótárdalur and Hóladalur (Figs. 1 and 2). In the Fremri-Grjótárdalur cirque, two lower relict rock glacier sectors have been differentiated, overlapped by active rock glaciers in the western and eastern sectors of the cirque (Andrés et al., 2016; Farbrot et al., 2007; Kellerer-Pirklbauer et al., 2007). The whole rock glacier complex occupies an area of 0.96 km^2 with a maximum length of 1 km and a maximum width of almost 300 m. These rock glaciers show typical features, i.e. transverse ridges and furrows composed of large angular boulders (Kellerer-Pirklbauer et al., 2007). The collapsed fronts of the relict rock glaciers descend to an altitude of 850 m a.s.l., while the steep fronts of the active ones descend to 950 m a.s.l. (Tanarro et al., 2018, 2019). The existence of interstitial ice in the active rock glaciers and the non-existence of ice in the relict rock glaciers have been demonstrated by geophysical surveys and field observations in previous works (Farbrot et al., 2007; Kellerer-Pirklbauer et al., 2007, Tanarro et al., 2018, 2019).

The Hóladalsjökull glacier, located in the adjacent cirque to the east of Fremri-Grjótárdalur (Fig. 1), is formed by a debris-covered lower section, 2 km long and 1.3 km-wide, covering an area of 2.2 km^2. The front is located at 900 m a.s.l. The upper sector is formed by 1.7 km-long debris-free glacial ice, occupying an area of 2.5 km^2

(Tanarro et al., 2018, 2019). Previous works described the existence of glacial ice, up to 20 m thick, under a meter-thick debris in the debris-covered sector of Hóladalsjökull glacier, which was visible at its forehead and in collapsed depressions (Andrés et al., 2016; Tanarro et al., 2018, 2019).

The age and origin of these rock glaciers and debris-covered glaciers is still under discussion. The ages of their inner and outer lobes age have been assumed to be between 5 and 9 ka for headwall recession rates estimation (Farbrot et al., 2007). Through streamline interpolations from present surface velocities, Wangensteen et al. (2006) estimated the maximum age of the rock glaciers to be about 4.5-5 ka BP, with reactivation of the higher lobes about 1.0-1.5 ka BP. Using a combination of the same method and Schmidt hammer dating, Kellerer-Pirklbauer et al. (2007, 2008) proposed an age contemporary with the 8.2 ka event (8.6-8.0 ka cal. yr BP according to Greenland stratigraphy; Alley and Ágústsdóttir, 2005) for Fremri-Grjótárdalur relict rock glaciers. Kellerer-Pirklbauer et al. (2007) proposed that the origin of the active rock glacier was related to one of the first neoglacial advances in Tröllaskagi at about 5.9-5.2 cal ka. BP, with reactivation during a second neoglacial advance by 3.2-3.0 ka (Kellerer-Pirklbauer et al., 2007). From a combination of headwall recession rate and lichenometric dating, the Nautárdalur rock glacier, located a few kilometers to the east, was considered to be about 0.2 ka old and related to the Little Ice Age glacial expansion (Martin et al., 1994; Hamilton and Whalley, 1995a, 1995b).

The dynamics of these rock and debris-covered glaciers are under discussion. Using data obtained by digital photogrammetry, Wangensteen et al. (2006), proposed horizontal block displacement rates ranging from less than 0.10 to a maximum of 0.84 m yr^{-1} in the Hóladalsjökull debris-covered glacier and a maximum of 0.74 m yr^{-1} in the Fremri-Grjótárdalur rock glacier. Kellerer-Pirklbauer et al. (2007) used similar

techniques in the Fremri-Grjótárdalur rock glacier and obtained rates of 0.06-0.74 m yr^{-1}. Lilleøren et al. (2013), used satellite radar interferometry and reported block displacement rates of 0.2–0.5 m yr^{-1} in some rock glaciers in Tröllaskagi. Tanarro et al. (2019) applied jointly manual and digital photogrammetry, obtaining a mean horizontal displacement rate of 0.33 m yr^{-1} for the Hóladalsjökull debris-covered glacier, mainly connected to surface lowering processes derived from ice degradation, and insignificant movement for the Fremri-Grjótárdalur rock glacier. These results are similar to those obtained in the Nautárdalur glacier, where boulder movement measured by theodolite during a 17-year period ranged from <0.05 m to 0.31 m yr^{-1}, with the snout advancing <1 m during this period (Whalley et al., 1995a, 1995b).

The second study area, Hofsjökull glacier, is located at the head of the Hofsdalur valley, to the south of Hólardalur (Fig. 1). Hofsjökull glacier is a 1.7 km long and 1.5 km wide debris-covered lower section and 1.3 km long debris-free upper section. Hofsjökull glacier has a thickness ratio of glacial ice and debris similar to Hóladalsjökull glacier (Campos et al., 2019). Campos et al. (2019) found average horizontal boulder displacement rates of 0.22 m yr^{-1} in Hofsjökull glacier, and 0.15 m yr^{-1} in the nearby Júllogil rock glacier, which confirms the stability of these glaciers whose predominant dynamic is the subsidence associated to ice downwasting.

The third study area is Héðinsdalsjökull in Héðinsdalur valley (Fig. 1), to the south of Hofsdalur. The distal sector of Héðinsdalsjökull is a debris mantle that evidences former extent of a debris-covered glacier. The snout of this palaeo debris-covered glacier is at 640 m a.s.l. The present debris-covered glacier extends from 900 m a.s.l. upwards, where ice-collapsed depressions can be observed on a debris mantle. The total debris-covered sector (with and without underlying ice) is 2.1 km long, with the collapsed and

active sectors being 1.2 and 0.9 km long, respectively. The upper sector is formed by debris-free glacial ice 2.3 km long and 2.6 km wide.

4. Methods

4.1 Geomorphological setting and CRE sampling strategy

The three complementary methodological steps of this research focused on the Fremri-Grjótárdalur rock glaciers and the Hóladalsjökull, Hofsjökull and Héðinsdalsjökull debris-covered glaciers. The first step was to determine when the deglaciation occurred in these valleys and in each of the two cirques. The second step was to determine the exposure age of the boulders of the relict rock glaciers located in the Fremri-Grjótárdalur cirque. In this context, the relict rock / fossil debris-covered glaciers are representative of the first landforms originated after deglaciation inside the cirques. The application of this strategy, following a clear chronological sequence indicated by the geomorphological landform disposition, will allow the reconstruction of the deglaciation phases and the rock glacier formation.

The final step was to determine the stabilization period of the frontal boulders of the debris-covered glaciers that still conserve underlying ice, and those without it. For sufficiently representative sampling, we took samples from boulders of both the Hofsjökull and Héðinsdalsjökull debris-covered glaciers. By this way, we will be able to deduce whether the stabilization moment of these debris-covered glaciers was synchronous in different valleys of Tröllaskagi.

Previous to CRE sampling of the fronts at the active debris-covered glaciers and rock glaciers, a photogrammetric analysis was applied to these boulders to measure their horizontal displacement and hence their stability degree in the last decades, in order to avoid that high-mobility or potentially overturned boulders are sampled.

Samples were taken from gentle flat-topped surfaces by using hammer and chisel, preferring boulders with a >1-m diameter and with signs of glacial polishing which minimize the risk of cosmogenic nuclide inheritance.

4.2 Movement analysis of the sampled boulders

To determine the degree of stability of the boulders sampled for CRE dating, we followed the method previously proposed by Tanarro et al. (2019). We applied digital photogrammetry to historical aerial photographs to determine the horizontal movement and elevation changes of sampled boulders from debris-covered glaciers and rock glaciers. This method was applied to the rock glacier in Fremri-Grjótárdalur, and the debris-covered glacier, the Hofsjökull, to complement previous analyses of boulder movement in the area (Tanarro et al., 2019; Campos et al., 2019). We used photo stereo pairs from 1980 and 1994, which were the only flights available with sufficient resolution quality to identify the same boulders in both years. The photo stereo pairs were scanned at a high resolution (20 and 15 microns respectively). A digital photogrammetric workstation was used to correct the geometric deformation of the photograms and to create stereoscopic models for both dates. In this process, the absolute orientation was obtained from a series of control points from an orthophoto of the year 2000. To estimate the uncertainty (RMSExyz) on the boulder tracking in rock glaciers and debris-covered glaciers, X, Y and Z values of moraine boulders that are considered stable and immobile were determined. The resulting RMSExyz values are at most 0.32 m. The photograms covering the area of the Fremri-Grjótárdalur and Hóladalsjökull cirques present a slightly lower error range (RMSExyz 0.15-0.25 m) than those covering the Hofsdalur cirque (RMSExyz 0.17-0.32 m). With the stereoscopic models from both dates, we carried out 3D photogrammetric restitution of a set of boulders identified on the surface of the sampled landforms (see the boulders

tracked and the geomorphological units to which they belong in Table 1). Some of these boulders were the same boulders as those sampled for CRE dating and others were very close to them in the same geomorphological unit (Figs. 2, 3 and 4). Finally, we compiled a database including X and Y coordinates, and altitude (Z) of each boulder in both dates. These data were then processed to obtain the horizontal displacement and elevation difference for each boulder.

4.3 ^{36}Cl CRE dating

The locations of the 18 CRE samples are shown in Table 2 and Figs. 3, 4 and 5. Samples HOL-1, HOL-2, FGD-1, FGD-2 and FGD-11 were collected during a fieldwork conducted in 2012. Preliminary results of these first samples were presented in Andres et al. (2016), but the age re-calculation with the new calculator (Schimmelpfennig et al., 2009) and different in situ ^{36}Cl production rates (detailed below) considerably improved the results. These samples were crushed and sieved in the "Physical Geography Laboratory" of the Complutense University of Madrid (Spain), and the 0.25-1 mm fraction was separated. Aliquots splits of rocks were taken for chemical analysis both from the pre-treated samples (bulk fraction; Table 3) and the samples after a first pre-dissolution conducing to the removal of Cl-rich ground mass (Table 4). Chemical analysis were carried out at the "Activation Laboratories" (Ancaster, Canada). Chemical processing of the samples was carried out at the "PRIME Laboratory" (Purdue University, USA), following the procedures described in Zreda et al. (1999) and Phillips (2003) for the ^{36}Cl extraction from whole rock. The resulting targets were analyzed using accelerator mass spectrometry (AMS) to determine the ^{35}Cl/^{37}Cl, ^{36}Cl/^{35}Cl and ^{36}Cl/^{37}Cl ratios. Two chemistry blanks (Cblk3125-1 and Cblk3125-2) were processed together with the samples, for which the laboratory

provided only the data collected in Table 5, with the previously calculated results of Cl and ^{36}Cl concentrations, which were used here to calculate the ^{36}Cl ages.

A second batch of samples, ELLID-1, ELLID-2, FGD-1B, FGD-2B, FGD-3B, FGD-4B, FGD-5B, HOFS-1, HOFS-2, HOFS-3, HEDIN-1, HEDIN-2 and HEDIN-3 were sampled in 2014 and 2015. The initial mechanical preparation was also carried out in the "Physical Geography Laboratory" (Complutense University of Madrid, Spain) and the 0.25-1 mm fraction was chemically processed in the Laboratoire National des Nucléides Cosmogéniques (LN_2C) at the "Centre Europeén de Recherche et d'Enseignement des Géosciences de l'Environnement" (CEREGE), in Aix-en-Provence (France). Aliquot splits of bulk rock were taken from several representative samples of each study area, in order to analyze the concentrations of major and trace elements (Table 3) at the "Service d'Analyse des Roches et des Mineraux" (SARM, Nancy, France). After removing dust and fines and etching the samples with nitric (HNO_3) and hydrofluoric (HF) acids, aliquots were taken again to measure the target element concentrations by inductively coupled plasma-optical emission spectrometer (ICP-OES) at SARM (Table 4). An ^{35}Cl-enriched spike (~99%) was then added to the samples for isotope dilution (Ivy-Ochs et al., 2004) and the samples were completely dissolved in a mixture of HF+HNO_3. The undissolved fines and fluoride gel was removed after centrifugation of the samples. The following steps of the process follow the procedure proposed by Schimmelpfennig et al. (2011). Finally, measurements of the $^{35}Cl/^{37}Cl$ and $^{36}Cl/^{35}Cl$ ratios were carried out at the "Accélérateur pour les Sciences de la Terre, Environnement et Risques" (ASTER, CEREGE), to infer the concentrations of ^{36}Cl and Cl. Three chemistry blanks (BK-1, BK-2 and BK-3) (Table 5) were processed together with the samples.

The Excel™ spreadsheet proposed by Schimmelpfennig et al. (2009) was used to calculate ^{36}Cl exposure ages. The most relevant data used in the calculations (topographic shielding factor, sample thickness, chemical composition of the samples) are summarized in Tables 2, 3 and 4. In absence of lab density measurements, a value of 2.7 g cm^{-3} is assumed for all samples. The nucleonic and muonic scaling factors based on the time-invariant "St" scheme (Stone, 2000) were applied, and the topographic shielding factor was calculated with the ArcGIS toolbox designed by Li (2018), since the data could not be taken directly in the field due to fog. The exposure age calculations were made with the following ^{36}Cl production rates: 57.3±5.2 atoms ^{36}Cl (g Ca)$^{-1}$ yr^{-1} for spallation of Ca (Licciardi et al., 2008), 148.1±7.8 atoms ^{36}Cl (g K)$^{-1}$ yr^{-1} for spallation of K (Schimmelpfennig et al., 2014), 13±3 atoms ^{36}Cl (g Ti)$^{-1}$ yr^{-1} for spallation of Ti (Fink et al., 2000), 1.9±0.2 atoms ^{36}Cl (g Fe)$^{-1}$ yr^{-1} for spallation of Fe (Stone et al., 2005), and 696±185 neutrons (g air)$^{-1}$ yr^{-1} for the production rate of epithermal neutrons from fast neutrons in the atmosphere at the land/atmosphere interface (Marrero et al., 2016). A high-energy neutron attenuation length of 160 g cm^{-2} was applied.

Table 5 shows ^{36}Cl CRE ages without erosion or snow cover corrections, together with the 1σ uncertainties including both the total error (including production rate errors) and the internal (analytical) error. In the text the ages are presented in ka rounded to one decimal place and with the analytical uncertainties to facilitate their comparison within our sample dataset.

5. Results

5.1 Movement of boulders from rock glaciers and debris-covered glaciers.

The results of the horizontal movement and elevation changes of the analyzed boulders are presented in Table 1. Their locations are shown in Figs. 2, 3 and 4.

The moraine boulders HOL-1 and HOL-2, located in the Hóladalsjökull cirque, have remained stable during the 14-year observation period. Horizontal movement (0.052 and 0.022 m yr^{-1}) and elevation changes (-0.04 and 0.06 m yr^{-1}) are negligible and within the RMSE of our analysis. We obtained similar results from the analysis of the moraine boulders in the Fremri-Grjótárdalur cirque, where sample FDG-11 was collected. There is the exception of one boulder, which indicates a slight horizontal movement of 0.108 m yr^{-1}, while the rest hardly show any movement, with maximum about 0.05 m yr^{-1}.

We obtained similar results from the boulders located on the ridges at the Fremri-Grjótárdalur relict rock glaciers. For example, in the western rock glacier from which samples FDG-1 and FDG-2 were collected, we obtained displacement rates of less than 0.047 m yr^{-1} and maximum elevation difference of -0.43 m yr^{-1}. In the eastern rock glacier, we obtained a movement of 0.022 m yr^{-1} for the samples FGD-4B and FGD-5B, and maximum elevation changes of -0.36 m yr^{-1}. In any case the total horizontal displacement during the 1980-1994 was not higher than 0.66 m (Table 1).

As it would be expected, different results were obtained from the boulders located on the ridges of the active rock glaciers (representative for samples FGD-1B, FGD-2B and FGD-3B), although the movement is very slow, between 0.076 m yr^{-1} and maximum 0.16 m yr^{-1}. These values, therefore, would indicate displacements of 1.06 and 2.2 m in 14 years. The elevation differences are negative, but negligible, between -0.04 and -0.19 m yr^{-1}.

We also obtained very small displacements on the front of the Hofsjökull debris-covered glacier (boulders from which samples HOFS-1, HOFS-2 and HOFS-3 were

collected). The horizontal displacement rates of the boulders range from 0.18 m to 0.37 m yr^{-1}, indicating about 2.5 and 5.16 m displacement and elevation changes of -0.19 to -1.26 m in 14 years.

5.2 Deglaciation of the Tröllaskagi internal valleys: geomorphology and CRE dating results.

Fieldwork and moraine mapping were carried out in the Víðinesdalur, Hofsdalur and Héðinsdalur valleys, during the summers of 2012, 2014 and 2015, exploring for erratic boulders or glacially polished bedrock surfaces suitable for applying CRE dating. The abundance of debris-flows and other slope processes have transformed and covered the glacial landforms of the valley. No bedrock outcrops, or any existing outstanding block in the relief were observed, with the exception of those generated by post-glacial rock avalanches. The only exceptions observed during the fieldwork were two polished bedrocks located on the Elliði ridge (Fig. 5), which separates the Víðinesdalur valley to the south from the Kolbeinsdalur valley to the north (Fig. 6). The polished surfaces are at around 600 m a.s.l., i.e. 300 m above the bottom of the Víðinesdalur valley. Samples were collected from each of these polished surfaces (ELLID-1 and ELLID-2), whose ages indicate the start of deglaciation of the studied valleys. Both samples gave very similar ages: 16.3 ± 1.2 ka (ELLID-1) and 16.3 ± 0.9 ka (ELLID-2), published in Fernández-Fernández et al. (2019).

5.3 Deglaciation of the Tröllaskagi cirques: geomorphology and CRE dating results.

To determine the timing of the deglaciation of the Fremri-Grjótárdalur and Hóladalsjökull cirques, glacial landforms located in front of the rock glaciers and the debris-covered glacier were studied. No polished surfaces are preserved, only remnants of a highly degraded moraine ridge in each cirque. In the Fremri-Grjótárdalur cirque there is a degraded lateral moraine in front of the rock glaciers (Figs. 2, 7 and 8). One

prominent glacial boulder (FDG-11) was considered suitable for exposure dating and yielded an age of 11.3±0.8 ka. A similar highly degraded moraine is located about 900 m distal and 100 m lower in altitude than the Hóladalsjökull debris-covered glacier (Fig. 9). Two large stable blocks with glacially polished surfaces were considered suitable for exposure dating (Fig. 9). From those, samples HOL-1 and HOL-2 yielded ages of 11.1±1.1 and 10.3±0.7 ka respectively (Figs. 6 and 9) (Figs. 6 and 9). The three ages are indistinguishable from each other within their 1 sigma analytical uncertainties, and are in chronostratigraphical order with the ELLID samples (Fig. 6).

5.4 Stabilization of boulders from the relict rock glaciers (without internal ice): geomorphology and CRE dating results.

Two large boulders (samples FDG-1 and FDG-2) were collected at the frontal margin of the relict rock glacier located below the active rock glaciers of the western sector of Fremri Grjótárdalur cirque about 870 m a.s.l. (Figs. 2, 7, 8). The samples yielded exposure ages of 10.5±0.7 and 11.1±0.7 ka respectively. Two more boulders (samples FDG-4B and FDG-5B) yielded ages of 9.3±0.7 and 9.5±0.7 ka respectively. They are located at the frontal edge of the other relict rock glacier at approximately 1005 m a.s.l., about 150 m higher than FDG-1 and FDG-2, in the eastern sector of the cirque (Fig. 2).

5.5 Stabilization of boulders from active rock glaciers and debris-covered glaciers (with stagnant internal ice): CRE dating results.

Three samples were collected from boulders at the front of the active rock glacier, with internal ice, to the western sector of Fremri-Grjótárdalur (FGD-1B, FGD-2B and FDG-3B), at an altitude of approx. 960 m (Figs. 2 and 8). These samples gave ages of 2.5±0.2, 5.2±0.4 and 6.5±0.5 ka respectively, in good chronostratigraphical agreement with previous samples of the cirque (moraine and relict rock glacier). To determine the timing of the stabilization of the debris-covered glaciers, three samples were taken from

boulders at the frontal part of the Hofsjökull debris-covered glacier, located at the bottom of Hofsdalur. The front of Hofsjökull presents a glacial ice wall of around 20 m, covered by a 2-m-thick debris mantle. Three samples were collected from boulders at the front of the glacier, located at about 900 m a.s.l. (HOFS-1, HOFS-2 and HOFS-3; Figs. 3 and 10). The results of these samples yielded ages of 5.4±0.5, 5.6±0.5 and 6.7±0.6 ka, respectively. These ages are similar to the samples FGD-2B and FDG-3B from the active rock glaciers.

Finally, three samples were taken from the debris-covered glacier of Héðinsdalur, in the distal sector of Héðinsdalsjökull, where no internal ice persists at present (HEDIN-1, HEDIN-2 and HEDIN-3), at about 650 m a.s.l. (Fig. 4 and 11), and yielded ages of 3.0±0.3, 2.6±0.3 and 2.2±0.2 ka respectively.

5.6. Chronological sequence summary.

The application of ^{36}Cl dating has revealed that the onset of the deglaciation in the main valleys Viðinesdalur and Kolbeinsdalur started around 16 ka. Subsequently, cirque glaciers of Fremri-Grjótárdalur and Hóladalur culminated in a last glacial advance or stillstand at 11 ka, when the moraine abandonment was definitive. Shortly afterwards, the relict rock glaciers of Fremri-Grjótárdalur stabilized in the cirques at around 11-9 ka, while the active debris-covered glacier of Hofsdalur and the rock glaciers of Fremri-Grjótárdalur stagnated at 7-5 ka. And finally, the definitive stabilization of the relict debris-covered glacier of Héðinsdalsjökull occurred at 3-2 ka.

6. Discussion

6.1 Deglaciation of the Tröllaskagi internal valleys and beginning of the formation of the rock glaciers and debris-covered glaciers into the cirques.

The intense degradation of the Tröllaskagi glacial landscape, due to slope mass movements together with the deposition of soil, fluvial, debris-flow and aeolian sediments, which have partly covered the slopes, greatly limits the possibility of obtaining a sufficient number of reliable CRE samples to map/reconstruct the deglaciation pattern of the three studied valleys. The only samples obtained from the Elliði ridge summits (ELLID-1, ELLID-2) yielded the same age (16.3±1.0 ka) (Fig. 6). This age may indicate the definitive retreat of the glaciers that descended through the Hóladalur valley. The datings of the moraine remains observed in the Fremri-Grjótárdalur and Hóladalur cirques yielded indistinguishable ages of 11.3±0.7, 11.1±1.0 and 10.3±0.7 ka (Fig. 6), which are around 5 ka younger than those from the Elliði ridge.

The results obtained in this study reflect a similar deglaciation pattern to that observed elsewhere in Iceland. In fact, the onset of the deglaciation in Iceland can be determined around 18.6 cal. ka BP, in concordance with the global sea level rise (Andrews et al 2000; Ingólfsson and Norðdahl 2001), which increased sharply during the Bølling interstadial (14.7 to 14.1 ka BP), when the Icelandic Ice Sheet IIS collapsed and retreated from the north (Norðdahl et al., 2008; Norðdahl and Ingólfsson, 2015; Pétursson et al., 2015).

The ages obtained in this study suggest that the retreat of the glaciers in Tröllaskagi coincided with the retraction of the main tongue of the IIS in this area, which flowed down from the highlands throughout the Skagafjörður fjord. This glacier retreated from the mouth of the fjord (161 km north of the present Hofsjökull ice-cap) in 15.9±1.2 ka, based on ^{36}Cl dating (Andrés et al., 2018b). This indicates that from the Bølling interstadial, the glaciers in the internal Tröllaskagi valleys and the Skagafjörður IIS outlet glacier were already disconnected. This may show that from the Allerød

interstadial (13.9-12.9 ka) at least some of the Tröllaskagi glaciers behaved as alpine glaciers, already disconnected from the IIS. The Tröllaskagi plateau therefore, may have remained ice-free, as it has been widely proposed (Ingólfsson, 1991; Norðdahl, 1991a, 1991b; Rundgren and Ingólfsson, 1999; Andres et al., 2016).

Data from lacustrine and marine sediments, and sea level changes, suggest a cold period and glacial advances at the end of the Bølling interstadial, around 14 cal. ka BP (Ingólfsson et al. 1997; Pétursson et al. 2015; Patton et al. 2017). However, probably due to the intense paraglacial erosive activity, there is no geomorphological evidence of that cold episode in the Víðinesdalur valley or in the Fremri-Grjótárdalur and Hóladalur cirques. Lake sediments from the Torfadalsvatn lake, on the Skagi peninsula (west of the Skagafjörður fjord), show that temperatures rose to current levels during the Allerød interstadial in the Skagafjörður area (Rundgren 1995, 1999; Rundgren and Ingólfsson 1999). The Tröllaskagi glaciers, might have retreated reaching their their minimum extent in their cirques during the Bølling interstadial.

After the Allerød interstadial, during the Younger Dryas, major degradation of the biosphere and increased amounts of sea-ice occurred in northern Iceland (Rundgren 1995, 1999; Xiao et al., 2017). The glacial outlets descending from the IIS, reoccupied the main fjords of northern Iceland up to their middle parts according to shoreline and tephra distribution (Pétursson et al., 2015). This deglaciation pattern has been confirmed in Skagafjörður with ^{36}Cl CRE ages of 12.7±0.9 and 11.9±0.9 ka BP for polished surfaces, when the front of the glaciers left the middle part of the fjord, 130 km from the current Hofsjökull ice cap (Andrés et al., 2018b). The last important advance or stagnation of the IIS outlets in northern Iceland was around 11 ka (Preboreal), when their fronts were located at the innermost parts of the fjords (Ingólfsson et al., 1997; Norðdahl and Einarsson, 2001; Norðdahl and Pétursson, 2005; Pétursson et al., 2015).

^{36}Cl CRE ages confirm the position of the outlet terminus close to the present shoreline in the Skagafjörður fjord (90 km from the current Hofsjökull ice-cap) at around 11 ka (Andrés et al., 2018b). This last glacial advance was immediately followed by an abrupt retreat until the disappearance of the IIS within the current limits of the glaciers (Kaldal and Víkingsson, 1990; Andrews et al., 2000; Norðdahl and Einarsson, 2001; Geirsdóttir et al., 2002, 2009; Larsen et al., 2012; Pétursson et al., 2015; Harning, et al., 2016). This has been also confirmed by CRE ^{36}Cl ages in Skagafjörður (Andrés et al., 2018b).

Samples FDG-11 (11.3 ± 0.7 ka) from the Fremri-Grjótárdalur moraine, and HOL-1 (11.1 ± 1.1 ka) and HOL-2 (10.3 ± 0.7, ka) from the moraine in front of Hóladalsjökull glacier (Fig. 6), may represent a glacial advance or glacial front stagnation in the Hóladalur valley during the Preboreal, around 11 ka, similar to that observed at the bottom of the fjords. After this, the Hóladalur glaciers must have retreated very quickly, as occurred in the nearby ice-caps (Andrés et al., 2018b), probably until the total disappearance of all the Icelandic glaciers at ~9 ka (Larsen et al., 2012; Geirsdóttir et al., 2018). This may also be the case of Drangajökull, in the NW (Harning et al., 2016; Anderson et al, 2018b). However, other studies have also suggested that Drangajökull persisted into the early-mid Holocene (Schomacker et al., 2016).

The ages of the moraine located in front of the Fremri-Grjótárdalur relict rock glaciers (~11.3 ka) and the frontal sector of these rock glaciers (~10.5-11 ka and ~9.4 ka) date to the Early Holocene (Table 4). Note that we do not report mean ages for the rock glacier front as they might have had different exposure histories. These dates demonstrate the rapid transformation of the small debris-free glaciers that occupied the cirque at the beginning of the Holocene into rock glaciers, whose fronts stabilized shortly afterwards. The surface boulders on the frontal area of these rock glaciers seemed to have stabilized rapidly, resulting in undisturbed exposure to cosmic radiation, otherwise younger and

less internally coherent ages would have been expected (Fig. 2). Hereafter, we will use the concept of "stabilization" along the discussion assuming that the duration between boulder emplacement and stabilization is insignificant compared to the age of the landforms. The different stabilization ages of the fronts of the western and eastern relict rock glaciers (~10.5-11 ka and ~9.4 ka) may be related to their different altitudes, located around 870 m a.s.l. and between 940-990 m a.s.l., respectively: in a warming tendency context, with permafrost altitude rising, the rock glaciers that first become inactive are the lowest (Fig. 8). The similarity of the boulder ages from the relict rock glaciers and those of the moraines makes us confident that the samples are not affected by cosmogenic nuclide inheritance from earlier exposure periods (Andrés et al., 2018b; Fernández-Fernández et al., 2019), which is shown to be an issue in other areas (e.g. Çiner et al., 2017).

The formation of rock glaciers relatively quickly after the retreat of the glacial fronts from youngest moraines in the cirques may indicate that they derive from the rapid transformation of debris-free glaciers during the final deglaciation stages. After that, their fronts, already evolved to those typical of the rock glaciers, stabilized shortly afterwards as they lost the internal ice (Humlum, 2000; Janke et al., 2015; Monnier and Kinnard, 2015; Andrés et al., 2016; and many others). CRE dating of frontal boulders from relict rock glaciers and glacial polished bedrock on which they are supported has demonstrated in many mountain ranges that rock glaciers usually formed shortly after deglaciation, followed by relatively rapid stabilization of their fronts. This process has been observed in several areas of the Iberian Peninsula, such as Sierra Nevada (Palacios et al., 2016a), Sierra de Guadarrama (Palacios et al., 2012), Sierra de la Demanda (Fernández-Fernández et al., 2017a), the Cantabrian Mountains (Rodríguez-Rodríguez et al., 2017), the Central Pyrenees (Palacios et al., 2017) and the Eastern Pyrenees

(Andrés et al., 2018a), and also in the British Isles (Ballantyne et al., 2009), the Alps (Hippolyte et al., 2009; Moran et al., 2016), the Karçal Mountains in Lesser Caucasus (Dede et al., 2017) and in the New Zealand Southern Alps (Winkler and Lambiel, 2018).

The rapid formation of debris-covered glaciers and rock glaciers at the end of deglaciation and the early stabilization of their fronts has a logical explanation in many mountains (Winkler and Lambiel, 2018), but especially in the Tröllaskagi valleys (Fig. 12). Deglaciation supposes the decompression of the upper part of the cirque walls from the glacier ice, accelerating paraglacial processes shortly after its deglaciation, as it has been observed in other studied mountains (Ballantyne, 2002, 2009; Mercier, 2008; Oliva et al., 2016). Intense paraglacial activity just after deglaciation has been proposed in many valleys of Tröllaskagi, and it has even been demonstrated by radiocarbon dating of several landslides (Mercier et al., 2013, 2017; Cossart et al., 2014; Coquin et al., 2015; Decaulne et al., 2016). The intense supply of material from the slopes derived from paraglacial activity can transform a retreating glacier into a rock glacier or debris-covered glacier (Johnson, 1980; Giardino and Vitek, 1988; Ackert, 1998; Janke et al., 2015; Anderson et al., 2018a; among others). In the same way, the end of paraglacial activity may involve stabilization of the rock glacier (Humlum, 2000; Deline et al., 2015; Anderson and Anderson, 2016). Our results show that relatively short time passed since the glaciers advanced and formed glacial moraines and the formation and the subsequent stabilization of rock glaciers. If we consider the uncertainty ranges of the moraine and relict rock glacier stabilization ages (see Fig. 2), this period might have lasted 2-4 ka as maximum. These results support the idea that rock glaciers form during the transformation of glaciers within paraglacial mountain landscape (Knight et al., 2018). However, to explore whether the interstitial ice of these rock glacier comes from

glacial ice, as we propose, or from aggradation ice requires other research methods. In that sense, the combination of the field geomorphological survey and chronological analysis with a fabric study (e.g. Ribolini et al., 2007) can shed more light on the formation of the rock glaciers.

6.2 The exposure age of boulders in active rock glaciers and debris-covered glaciers and the climatic and geomorphological significance.

The CRE dating results from the front of the Fremri-Grjótárdalur rock glacier yielded ages of 6-2 ka (Table 5, Fig. 2 and 8), with two boulders around 6-5 ka. In the view of the results of boulder tracking (Table 1; Tanarro et al., 2019), which point to an evident stagnant state (<0.66 m of horizontal displacement in 14 years), the scatter of ages might be related to the ice melting and subsidence. If we consider that sampled boulders are located in a lower sector of the rock glacier, where the potential ice melting should be higher due to the higher temperature, the probability that a boulder overturned as the ice melted is cannot be ruled out completely. This rock glacier is considered active (Farbrot et al., 2007; Wangensteen et al., 2006; Kellerer-Pirklbauer et al., 2007, 2008). In a recent study, the mobility of its blocks was restricted to less than 0.15 m yr^{-1} of horizontal displacement and -0.37 m in sinking during 14 years (Tanarro et al., 2019). Our results show also limited horizontal movement rates of the boulders. For example, the highest displacement value for a boulder of Hosfdalur debris covered glacier is 5.16 m in 14 years, which means a displacement of 0.37 m yr^{-1}. In the case of Fremri-Grjótárdalur, the highest displacement value for a block is 2.2 m, that is, 0.16 m yr^{-1} (Table 1). Other authors have obtained higher values in these same rock glaciers, but with automatic digital photogrammetry. Specifically, these authors propose 0.6 m yr^{-1} to 0.74 m yr^{-1} (Kellerer-Pirklbauer et al., 2007) or 0.07 m yr^{-1} to 0.89 m yr^{-1} (Wangensteen et al., 2006). On the contrary, the values obtained in this work are similar to those

obtained by direct observation through total station in Nautárdalur rock glacier, also in Tröllaskagi, with values between 0.2 m yr^{-1} to 0.25 m yr^{-1} (Whalley et al., 1995). Our results would be within the range of rock glaciers of very low activity, for example, among those studied in the Alps, where movements have been measured from a few cm yr^{-1} up to 10 m yr^{-1} (Delaloye et al., 2010). Previous work has shown that the boulders with greatest horizontal displacement in the debris covered glaciers are also those that have had the greatest sinking (Tanarro et al., 2019; Campos et al., 2019). The morphology of these formations has not changed in 50 years, which suggests that the surface of these formations is sinking uniformly. As a consequence of this process and the location of the tracked boulders in a gentle slope, the dynamics observed point to a slight horizontal displacement (Tanarro et al., 2019; Campos et al., 2019). It is important to consider that both rock glaciers and debris covered glaciers are approximately at the limit of permafrost (Wangensteen et al., 2006; Etzelmüller et al., 2007; Czekirda et al., 2019), probably in thermal conditions in which the layer of debris is sufficient to insulate the internal ice from radiation, although in fact there is no accretion of permafrost. In the view of the limited mobility of the active rock glaciers and debris-covered glaciers and their predominant subsidence dynamics, it seems to be evident that they have no longer accumulate ice in their headwall areas (accumulation zone).

Our information obtained about the almost null flow of these formations is limited to the last decades, in agreement with previous works (Tanarro et al., 2019; Campos et al., 2019). This practically null movement occurs while interstitial ice is present inside the studied rock glaciers. In the case of the debris-covered glaciers, the glacial ice is covered by a thin layer of debris, around one meter thick (Farbrot et al., 2007; Kellerer-Pirklbauer et al., 2007; Andrés et al., 2018; Tanarro et al., 2019; Campos et al., 2019).

However, despite of this movement, no change in the morphology of both rock glaciers and debris-covered glaciers has been detected in the last fifty years (Tanarro et al., 2019; Campos et al., 2019), except for the formation of thermokarst depressions indicative of a slow ice melting.

We assume that, despite the debris-covered and rock glaciers still contain internal ice, they have had a very limited or almost null flow the last thousands of years, otherwise boulders would have moved and overturned and consequently, their dated surfaces would not have been constantly exposed to cosmic radiation. If these formations had experienced an important flow with boulder toppling, the exposure ages of the sampled boulders would be much younger and less coherent. However, all our dated surfaces are chronologically coherent, except sample FDG-1B, which is 3-4 ka younger than the two adjacent boulders, probably due to an overturning. These results support that the Hólar debris-covered and rock glaciers have been static for a long period and that consequently, most of the sampled surfaces of their boulders have been continuously exposed to cosmic radiation without disturbances (e.g. overturning) continuously during the last 5 ka. As a suggestion, this date of definitive stabilization could reflect the impact of the Holocene Thermal Maximum (HTM), which in Tröllaskagi entailed the maximum birch expansion between 8 and 5 ka BP, with temperatures higher than at present (1961-1990 series) (Wastl et al., 2001; Caseldine et al., 2006). According to lake sediment dating, the ice cap Drangajökull glacier, in northeast Iceland, had retreated compared to its current extent (Schomacker et al., 2016) or even disappeared (Harning et al., 2016, 2018) at that time, just as other central ice-caps (Anderson et al., 2018b; Geirsdóttir et al., 2018). A MAAT >3ºC above the present mean value would be required for this to occur (Anderson et al., 2018b; Geirsdóttir et al., 2018). We can therefore deduce that the Fremri-Grjótárdalur rock glacier flow ended during the HTM,

when the headland glacier stopped feeding the tongue, composed of a mixture of debris and ice, which remained static, as it was above the permafrost level in this period (Etzelmüller et al., 2007; Wangensteen et al., 2006).

Nevertheless, with our data another interpretation is possible. The present Tröllaskagi rock glaciers with internal ice could have been formed at the onset of the Neoglacial cooling, 5 ka ago (see synthesis in Geirsdóttir et al., 2018). However, more subsurface data of the active rock glaciers (e.g. ice petrography) would be needed to prove the origin of the internal ice: past glaciers or ice formed under permafrost conditions (Ribolini et al., 2007). Moreover, if the origin of interstice ice in the rock glacier had been related to the accretion of ice in permafrost conditions, more time would have been necessary for its formation before its early stabilization.

The comparison of our results with other cases is complicated, since the boulders on the top of an active rock glacier (Fig. 12) have only been dated very rarely, e.g. by Winkler and Lambiel, 2018 (Southern Alps) with the Schmidt-Hammer method, and on the basis of a calibration curve reconstructed with the help of CRE-dated boulders of an adjacent moraine. This work supports our hypothesis according to which the CRE ages from the rock glacier boulders would be indicating the age of the rock glacier stabilization.

The results obtained in the Hofsjökull debris-covered glacier are similar to those of the stagnant active rock glaciers in Fremri-Grjótárdalur. Three boulders at the glacier front yielded similar ages of 7-5 ka, thus supporting its possible “stabilization” during the HTM. It is important to remember that these blocks belong to a 2 m thick debris cover, resting on about 20 m thick glacial ice. Their current boulder subsidence rate is of -0.55 m yr^{-1} and the horizontal displacement ranges from 0.18 to 0.37 m yr^{-1}, probably derived from the subsidence processes, and their frontal limits did not advance over the past 50 years.

The CRE results obtained from the collapsed sector of the Héðinsdalsjökull debris-covered glacier, at 650 m a.s.l., yielded ages between 3 and 2 ka. This front is now completely static and has no internal ice. We assume that these boulders could easily rotate when the glacier ice melted, and therefore their cosmogenic age shows the time that they have been stable since then. CRE dates previously obtained on fossil debris-covered glaciers suggest different durations of existence when these glaciers are exposed to strong solar radiation and thus lost the ice shortly after being formed, compared to nearby glaciers which are more shielded, with glacial activity lasting for thousands of years (Fernández-Fernández et al., 2017a). Thus, our results may show the end of some Neoglacial advances in Tröllaskagi around 3.2 ka (Caseldine and Hatton, 1994; Stötter et al., 1999; Wastl et al., 2001 among others), as it occurred in some sectors of Drangajökull (Harning et al., 2016, 2018), where lake records indicate severe cooling in Iceland (synthesis in Geirsdóttir et al., 2018).

7. Conclusions.

Our results allow a preliminary reconstruction of the glacier behavior in valleys and cirques of the Tröllaskagi peninsula during and after the last deglaciation. The deglaciation of the main valleys (Viðinesdalur and Kolbeinsdalur) in the Tröllaskagi peninsula began their retreat at around 16 ka. The glacier dynamics between the onset of deglaciation and the beginning of the Holocene cannot be determined at present, as in our study area no glacial landforms are preserved between the terminal part of the valleys and the base of the cirques. Small moraines exist in these cirques, with ages apparently corresponding to the last glacial advance in the fjords, probably during the Preboreal, around 11 ka. After this date, the glaciers retreated and temperatures rose abruptly, as in the rest of Iceland, triggering paraglacial processes on the deglaciated walls, including gravitational events, with the subsequent formation of debris-covered

and rock glaciers whose fronts shortly after stabilized, especially those at lower altitudes.

New rock glaciers and debris-covered glaciers were then formed at the upper sectors of the valleys sometime after the Preboreal. These new formations still retain currently internal ice covered by debris. Moreover, they display minimal dynamics, mainly related to subsidence. These limited dynamics allowed most of the boulder surfaces resting on the ice to be continuously exposed to cosmic radiation. This indicates that these debris-covered glaciers and rock glaciers no longer accumulated ice in their head areas. This stabilization timing oscillates between 7 and 3 ka ago and may have been caused either by the HTM warm period or remobilization during the cold Neoglacial periods. Thus, this research demonstrates the potential of CRE dating methods in the study of the past dynamics of debris-covered glaciers and rock glaciers both in the frame of the glacial landscape evolution and in the understanding of the debris-free glaciers transformation to debris-covered and rock glaciers. However, to fully understand this evolution and its origin, more information must be collected both from other nearby rock glaciers or debris-covered glaciers to have a more complete overview and more representative study cases in a statistical point of view. Subsurface data would also have a great potential as internal ice of rock glacier and debris-covered glaciers is not present homogeneously in the detrital bodies, and this information would complement the conclusions derived from the boulder mobility/stability analysis.

Acknowledgements

This paper was funded by the project CGL2015-65813-R (Spanish Ministry of Economy and Competitiveness) and Nils Mobility Program (EEA GRANTS), and with the help of the High Mountain Physical Geography Research Group (Complutense University of Madrid). We thank the Icelandic Association for Search and Rescue, the

Icelandic Institute of Natural History, the Hólar University College, and David Palacios Jr. and María Palacios for their support in the field. José M. Fernández-Fernández received a PhD fellowship from the FPU programme (Spanish Ministry of Education, Culture and Sport; reference FPU14/06150). The ^{36}Cl measurements were performed at the ASTER AMS national facility (CEREGE, Aix-en-Provence), which is supported by the INSU/CNRS and the ANR through the "Projets thématiques d'excellence" program for the "Equipements d'excellence" ASTER-CEREGE action and IRD. The authors express their deep gratitude to Dr. Adriano Ribolini and an anonymous reviewer, whose corrections and suggestions have contributed significantly to improve the earlier draft of the manuscript and figures.

References

Ackert, jr., R.P., 1998. A rock glacier/debris- covered glacier system at Galena Creek, Absaroka mountains, Wyoming. Geogr. Ann. Ser. A, Phys. Geogr. 80, 267–276. https://doi.org/10.1111/j.0435-3676.1998.00042.x

Alley, R.B., Ágústsdóttir, A.M., 2005. The 8k event: Cause and consequences of a major Holocene abrupt climate change. Quat. Sci. Rev. 24, 1123–1149. https://doi.org/10.1016/j.quascirev.2004.12.004

Anderson, L.S., Anderson, R.S., 2016. Modeling debris-covered glaciers: response to steady debris deposition. Cryosph. 10, 1105–1124. https://doi.org/10.5194/tc-10-1105-2016

Anderson, L.S., Flowers, G.E., Jarosch, A.H., Aðalgeirsdóttir, G.T., Geirsdóttir, Á., Miller, G.H., Harning, D.J., Thorsteinsson, T., Magnússon, E., Pálsson, F., 2018b. Holocene glacier and climate variations in Vestfirðir, Iceland, from the modeling of

Drangajökull ice cap. Quat. Sci. Rev. 190, 39–56. https://doi.org/10.1016/j.quascirev.2018.04.024

Anderson, R.S., Anderson, L.S., Armstrong, W.H., Rossi, M.W., Crump, S.E., 2018a. Glaciation of alpine valleys: The glacier–debris-covered glacier–rock glacier continuum. Geomorphology 311, 127-142. https://doi.org/10.1016/j.geomorph.2018.03.015.

Andrés, N., Gómez-Ortiz, A.., Fernández-Fernández, J.M., Tanarro, L.M., Salvador-Franch, F., Oliva, M., Palacios, D., 2018a. Timing of deglaciation and rock glacier origin in the southeastern Pyrenees: a review and new data. Boreas. https://doi.org/10.1111/bor.12324

Andrés, N., Palacios, D., Saemundsson, Þ., Brynjólfsson, S., Fernández-Fernández, J.M., 2018b. The rapid deglaciation of the Skagafjörður fjord, northern Iceland. Boreas. https://doi.org/10.1111/bor.12341

Andrés, N., Tanarro, L.M., Fernández, J.M., Palacios, D., 2016. The origin of glacial alpine landscape in Tröllaskagi Peninsula (North Iceland). Cuad. Investig. Geográfica 42 (2), 341-368. http://dx.doi.org/10.18172/cig.2935.

Andrews, J.T., Harðardóttir, J., Helgadóttir, G., Jennings, A.E., Geirsdóttir, Á., Sveinbjörnsdóttir, Á.E., Schoolfield, S., Kristjánsdóttir, G.B., Smith, L.M., Thors, K., Syvitski, J., 2000. The N and W Iceland Shelf: Insights into Last Glacial Maximum ice extent and deglaciation based on acoustic stratigraphy and basal radiocarbon AMS dates. Quat. Sci. Rev. 19, 619-631. https://doi.org/10.1016/S0277-3791(99)00036-0

Azócar, G., Brenning, A., 2010. Hydrological and geomorphological significance of rock glaciers in the dry Andes, Chile (27º-33ºS). Permafr. Periglac. Process. 21 (1), 42-53. http://dx.doi.org/10.1002/ppp.669.

Bachrach, T., Jakobsen, K., Kinney, J., Nishimura, P., Reyes, A., Laroque, C.P., Smith, D.J., 2004. Dendrogeomorphological assessment of movement at Hilda rock glacier, Banff National Park, Canadian Rocky Mountains. Geogr. Ann., 86 A (1): 1–9.

Ballantyne, C.K., Schnabel, Ch., Xu, S., 2009. Exposure dating and reinterpretation of coarse debris accumulations (‘rock glaciers’) in the Cairngorm Mountains, Scotland. J. Quat. Sci. 24, 19-31. https://doi.org/10.1002/jqs.1189

Ballantyne, C.K., 2013. Paraglacial Geomorphology, in: Encyclopedia of Quaternary Science: Second Edition. Elsevier, pp. 553–565. https://doi.org/10.1016/B978-0-444-53643-3.00089-3

Barsch, D., 1996. Rock Glaciers. Springer, Berlin, 331 pp.

Benedict, J.B. 1973. Chronology cirque glaciation, Colorado Front Range. Quat. Res. 3, 584-599. https://doi.org/10.1016/0033-5894(73)90032-X

Benn, D.I., Bolch, T., Hands, K., Gulley, J., Luckman, A., Nicholson, L.I., Quincey, D., Thompson, S., Toumi, R., Wiseman, S., 2012. Response of debris-covered glaciers in the Mount Everest region to recent warming, and implications for outburst flood hazards. Earth-Science Rev. 114, 156–174. https://doi.org/10.1016/j.earscirev.2012.03.008

Berger, J., Krainer, K., Mostler, W., 2004. Dynamics of an active rock glacier (Ötztal Alps, Austria). Quat. Res. 62, 233–242. https://doi.org/10.1016/J.YQRES.2004.07.002

Bibby, T., Putkonen, J., Morgan, D., Balco, G., Shuster, D.L., 2016. Million year old ice found under meter thick debris layer in Antarctica. Geophys. Res. Lett. 43 (13), 6995e7001. http://dx.doi.org/10.1002/2016GL069889.

Björnsson, H., Pálsson, F., 2008. Icelandic glaciers. Jökull 58, 365–386.

Bosson, J.B., Lambiel, C., 2016. Internal Structure and Current Evolution of Very Small Debris-Covered Glacier Systems Located in Alpine Permafrost Environments. Front. Earth Sci. 4. https://doi.org/10.3389/feart.2016.00039

Brenning, A., 2005. Geomorphological, hydrological and climatic significance of rock glaciers in the Andes of Central Chile (33-35°S). Permafr. Periglac. Process. 16, 231–240. https://doi.org/10.1002/ppp.528

Briner, J. P., Tulenko, J. P., Young, N. E., Baichtal, J. F., & Lesnek, A., 2017. The last deglaciation of Alaska. Cuadernos de Investigación Geográfica, 43(2), 429-448. http://dx.doi.org/10.18172/cig.3229

Brynjólfsson, S., Schomacker, A., Ingólfsson, Ó., Keiding, J.K., 2015. Cosmogenic 36Cl exposure ages reveal a 9.3 ka BP glacier advance and the Late Weichselian-Early Holocene glacial history of the Drangajökull region, northwest Iceland. Quat. Sci. Rev. 126, 140–157. doi:10.1016/j.quascirev.2015.09.001

Campos, N., Tanarro, L.M., Palacios, D., Zamorano, J.J., 2019. Slow dynamics in debris-covered and rock glaciers in Hofsdalur, Tröllaskagi Peninsula (northern

Iceland). Geomorphology 342, 61–77. https://doi.org/10.1016/j.geomorph.2019.06.005

Capt, M., Bosson, J.B.B., Fischer, M., Micheletti, N., Lambiel, C., 2016. Decadal evolution of a very small heavily debris-covered glacier in an Alpine permafrost environment. J. Glaciol. 62, 535–551. https://doi.org/10.1017/jog.2016.56

Caseldine, C., Hatton, J., 1994. Environmental change in Iceland. Münchener Geogr. Abhandlungen. R. B Bd. B 12 41–62.

Caseldine, C., Langdon, P.G., Holmes, N. 2006. Early Holocene climate variability and the timing and extent of the Holocene thermal maximum (HTM) in northern Iceland. Quat. Sci. Rev. 25, 2314-2331. https://doi.org/10.1016/j.quascirev.2006.02.003

Caseldine, C., Stötter, J., 1993. "Little Ice Age" glaciation of Tröllaskagi peninsula, northern Iceland: climatic implications for reconstructed equilibrium line altitudes (ELAS). The Holocene 3, 357–366. https://doi.org/10.1177/095968369300300408

Caseldine, C.J., 1985. The Extent of Some Glaciers in Northern Iceland during the Little Ice Age and the Nature of Recent Deglaciation. Geogr. J. 151, 215–227. https://doi.org/10.2307/633535

Czekirda, J., Westermann, S., Etzelmüller, B., & Jóhannesson, T. (2019). Transient modelling of permafrost distribution in Iceland. Frontiers in Earth Science, 7, 130. https://doi.org/10.3389/feart.2019.00130

Çiner, A., Sarikaya, M.A., Yildirim, C., 2017. Misleading old age on a young landform? The dilemma of cosmogenic inheritance in surface exposure dating: Moraines vs.

rock glaciers. Quaternary Geochronology 42, 76-88. https://doi.org/10.1016/j.quageo.2017.07.003

Clark, D.H., Clark, M.M., Gillespie, A.R., 1994. Debris-covered glaciers in the Sierra Nevada, California, and their implications for snowline reconstructions. Quat. Res. https://doi.org/10.1006/qres.1994.1016

Coquin, J., Mercier, D., Bourgeois, O., Cossart, E., Decaulne, A., 2015. Gravitational spreading of mountain ridges coeval with Late Weichselian deglaciation: Impact on glacial landscapes in Tröllaskagi, northern Iceland. Quat. Sci. Rev. 107, 197–213. doi:10.1016/j.quascirev.2014.10.023

Cossart, E., Mercier, D., Decaulne, A., Feuillet, T., Jónsson, H.P., Saemundsson, Þ., 2014. Impacts of post-glacial rebound on landslide spatial distribution at a regional scale in northern Iceland (Skagafjörður). Earth Surf. Process. Landforms 39, 336–350. https://doi.org/10.1002/esp.3450

Crochet, P., Jóhannesson, T., Jónsson, T., Sigurðsson, O., Björnsson, H., Pálsson, F., Barstad, I., 2007. Estimating the Spatial Distribution of Precipitation in Iceland Using a Linear Model of Orographic Precipitation. J. Hydrometeorol. 8, 1285–1306. https://doi.org/10.1175/2007JHM795.1

Decaulne, A., Cossart, E., Mercier, D., Feuillet, T., Coquin, J., Jónsson, H.P., 2016. An early Holocene age for the Vatn landslide (Skagafjörður, central northern Iceland): Insights into the role of postglacial landsliding on slope development. The Holocene 26, 1304-1318. https://doi.org/10.1177/0959683616638432

Dede, V., Cicek, I., Sarikaya, M. A., Ciner, A., Uncu, L., 2017. First cosmogenic geochronology from the Lesser Caucasus: late Pleis- tocene glaciation and rock

glacier development in the Karçal Valley, NE Turkey. Quat. Sci. Rev. 164, 54–67. https://doi.org/10.1016/j.quascirev.2017.03.025

Delaloye, R., Perruchoud, E., Avian, M., Kaufmann, V., Bodin, X., Hausmann, H., Ikeda, A., Kääb, A., Kellerer-Pirklbauer, A., Krainer, K., Lambiel, C., Mihajlovic, D., Staub, B., Roer, I., Thibert, E., 2008. Recent Inter annual Variations of Rock Glacier Creep in the European Alps, in: Ninth International Conference on Permafrost. Fairbanks, Alaska, United States, pp. 343–348.

Delaloye, R., Lambiel, C., Gärtner-Roer, I., 2010. Overview of rock glacier kinematics research in the Swiss Alps. Geographica Helvetica, 65 (2), 135- 145.

Deline, P., Akçar, N., Ivy-Ochs, S., Kubik, P.W., 2015. Repeated Holocene rock avalanches onto the Brenva Glacier, Mont Blanc massif, Italy: A chronology. Quat. Sci. Rev. 126, 186-200 http://dx.doi.org/10.1016/j.quascirev.2015.09.004

Emmer, A., Loarte, E.C., Klimeš, J., Vilímek, V., 2015. Recent evolution and degradation of the bent Jatunraju glacier (Cordillera Blanca, Peru). Geomorphology 228, 345–355. https://doi.org/10.1016/J.GEOMORPH.2014.09.018

Eriksen, H.Ø., Rouyet, L., Lauknes, T.R., Berthling, I., Isaksen, K., Hindberg, H., Corner, G.D., 2018. Recent Acceleration of a Rock Glacier Complex, Ádjet, Norway, Documented by 62 Years of Remote Sensing Observations. Geophysical Research Letters 45 (16), 8314-8323. https://doi.org/10.1029/2018GL077605

Etzelmüller, B., Farbrot, H., Guðmundsson, Á., Humlum, O., Tveito, O.E., Björnsson, H., 2007. The regional distribution of mountain permafrost in Iceland. Permafr. Periglac. Process. 18, 185–199. https://doi.org/10.1002/ppp.583

Farbrot, H., Etzelmüller, B., Guðmundsson, Á., Humlum, O., Kellerer-Pirklbauer, A., Eiken, T., Wangensteen, B., 2007. Rock glaciers and permafrost in Tröllaskagi, northern Iceland. Z. Geomorph. N.F. (Suppl. 51), 1–16. https://doi.org/10.1127/0372-8854/ 2007/0051S2-0001

Fernández-Fernández, J.M., Andrés, N., Sæmundsson, Þ., Brynjólfsson, S., Palacios, D., 2017b. High sensitivity of North Iceland (Tröllaskagi) debris-free glaciers to climatic change from the 'Little Ice Age' to the present. The Holocene 27, 1187–1200. https://doi.org/10.1177/0959683616683262

Fernández-Fernández, J.M., Palacios, D., García-Ruiz, J.M., Andrés, N., Schimmelpfennig, I., Gómez-Villar, A., Santos-González, J., Álvarez-Martínez, J., Arnáez, J., Úbeda, J., Léanni, L., Aumaître, G., Bourlès, D., Keddadouche, K., 2017a. Chronological and geomorphological investigation of fossil debris-covered glaciers in relation to deglaciation processes: A case study in the Sierra de La Demanda, northern Spain. Quat. Sci. Rev. 170, 232–249. https://doi.org/10.1016/j.quascirev.2017.06.034

Fernández-Fernández, J.M., Palacios, D., Andrés, N., Schimmelpfennig, I., Brynjólfsson, S., Sancho, L.G., Zamorano, J.J., Heiðmarsson, S., Sæmundsson, Þ., 2019. A multi-proxy approach to Late Holocene fluctuations of Tungnahryggsjökull glaciers in the Tröllaskagi peninsula (northern Iceland). Sci. Total Environ. 664, 499–517. https://doi.org/10.1016/j.scitotenv.2019.01.364

Feuillet, T., Coquin, J., Mercier, D., Cossart, E., Decaulne, A., Jónsson, H.P., Sæmundsson, Þ., 2014. Focusing on the spatial non-stationarity of landslide predisposing factors in northern Iceland. Prog. Phys. Geogr. 38, 354–377. https://doi.org/10.1177/0309133314528944

Fink, D., Vogt, S., Hotchkis, M., 2000. Cross-sections for 36Cl from Ti at Ep=35–150 MeV: Applications to in-situ exposure dating. Nucl. Instruments Methods Phys. Res. Sect. B Beam Interact. with Mater. Atoms 172, 861–866. doi:10.1016/S0168-583X(00)00200-7

Fuchs, M.C., Bohlert, R., Krbetschek, M., Preusser, F., Egli, M., 2013. Exploring the potential of luminescence methods for dating Alpine rock glaciers. Quat. Geochronol. 18, 17-33. http://dx.doi.org/10.1016/j.quageo.2013.07.001.

Galanin, A.A. Lytkin, V.M. Fedorov, A.N. Kadota, T. 2014, Kriosfera Zemli, XVIII (2), 64–74.

Geirsdóttir, Á., Andrews, J.T., Ólafsdóttir, S., Helgadóttir G., Harðardóttir J., 2002. A 36 Ky record of iceberg rafting and sedimentation from north-west Iceland. Polar Research 21, 291-298. https://doi.org/10.3402/polar.v21i2.6490

Geirsdóttir, Á., Miller, G.H., Andrews, J.T., Harning, D.J., Anderson, L.S., Thordarson, T., 2018. The onset of Neoglaciation in Iceland and the 4.2 ka event. Clim. Past Discuss. 1–33. https://doi.org/10.5194/cp-2018-130

Geirsdóttir, Á., Miller, G.H., Axford, Y., Ólafsdóttir, S., 2009. Holocene and latest Pleistocene climate and glacier fluctuations in Iceland. Quat. Sci. Rev. 28, 2107–2118. https://doi.org/10.1016/j.quascirev.2009.03.013

Giardino, J.R., Vitek, J.D., 1988. The significance of rock glaciers in the glacial periglacial landscape continuum. J. Quat. Sci. 3 (1), 97-103. http://dx.doi.org/10.1002/jqs.3390030111

Gibson, M.J., Glasser, N.F., Quincey, D.J., Rowan, A.V., Irvine-Fynn, T.D., 2017. Changes in glacier surface cover on Baltoro glacier, Karakoram, north Pakistan, 2001–2012. J. Maps 13, 100–108. https://doi.org/10.1080/17445647.2016.1264319

Glasser, N.F., Jansson, K.N., Duller, G.A.T., Singarayer, J., Holloway, M., Harrison, S., 2016. Glacial lake drainage in Patagonia (13–8 kyr) and response of the adjacent Pacific Ocean. Sci. Rep. 6, 21064.

Haeberli, W., Brandova, D., Burga, C., Egli, M., Frauenfelder, R., Kääb, A., Maisch, M., Mauz, B., Dikau, R., 2003. Methods for absolute and relative age dating of rockglacier surfaces in alpine permafrost. In: Phillips, M., Springman, S., Arenson, L. (Eds.), Proceedings of the 8th International Conference on Permafrost 2003, Zürich, pp. 343-348. http://www.arlis.org/docs/vol1/ICOP/55700698/Pdf/Chapter_062.pdf.

Haeberli, W., Hallet, B., Arenson, L., Elconin, R., Humlum, O., Kääb, A., Kaufmann, V., Ladanyi, B., Matsuoka, N., Springman, S., Vonder Mühll, D., 2006. Permafrost creep and rock glacier dynamics. Permafr. Periglac. Process. 17 (3), 189-214. http://dx.doi.org/10.1002/ppp.561.

Hambrey, M.J., Quincey, D.J., Glasser, N.F., Reynolds, J.M., Richardson, S.J., Clemmens, S., 2008. Sedimentological, geomorphological and dynamic context of debris-mantled glaciers, Mount Everest (Sagarmatha) region, Nepal. Quat. Sci. Rev. 27, 2361–2389. https://doi.org/10.1016/j.quascirev.2008.08.010

Hamilton, S.J., Whalley, W.B., 1995a. Preliminary results from the lichenometric study of the Nautardalur rock glacier, Tröllaskagi, northern Iceland. Geomorphology 12, 123–132. https://doi.org/10.1016/0169-555X(94)00083-4

Hamilton, S.J., Whalley, W.B., 1995b. Rock glacier nomenclature: a re-assessment. Geo- morphology 14, 73–80. https://doi.org/10.1016/0169-555X(95)00036-5.

Harning, D.J., Geirsdóttir, Á., Miller, G.H., Zalzal, K., 2016. Early Holocene deglaciation of Drangajökull, Vestfirðir, Iceland. Quat. Sci. Rev. 153, 192–198. doi:10.1016/j.quascirev.2016.09.030

Harning, D.J., Thordarson, T., Geirsdóttir, Á., Zalzal, K., Miller, G.H., 2018. Provenance, stratigraphy and chronology of Holocene tephra from Vestfirðir, Iceland. Quat. Geochronol. 46, 59–76. https://doi.org/10.1016/J.QUAGEO.2018.03.007

Hippolyte, J.C., Bourlès, D., Braucher, R., Carcaillet, J., Léanni, L., Arnold, M., Aumaitre, G., 2009: Cosmogenic 10Be dating of a sackung and its faulted rock glaciers, in the Alps of Savoy (France). Geomorphology 108, 312-320 http://www.springer.com/us/book/9783642800955.

Hubbard, A., Sugden, D., Dugmore, A., Norddahl, H., Pétursson, H.G., 2006. A modelling insight into the Icelandic Last Glacial Maximum ice sheet. Quat. Sci. Rev. 25, 2283–2296. https://doi.org/10.1016/J.QUASCIREV.2006.04.001

Humlum, O., 1998. The climatic significance of rock glaciers. Permafr. Periglac. Process. 9, 375–395. https://doi.org/10.1002/(SICI)1099-1530(199810/12)9:4<375::AID-PPP301>3.0.CO;2-0

Humlum, O., 2000. The geomorphic significance of rock glaciers: estimates of rock glacier debris volumes and headwall recession rates in West Greenland. Geomorphology 35, 41–67. https://doi.org/10.1016/S0169-555X(00)00022-2

Icelandic Meteorological Office, 2018. Climatological data. Available on http//en.vedur.is/climatology/data/ (accessed 13 April 2018).

Ingólfsson, O., 1991. A review of the late Weichselian and early Holocene glacial and environmental history of Iceland. In: J. Maizels, C. Caseldine (eds.), Environmental Change in Iceland: Past and Present, Kluwer Academic Publishers, Dordrecht, pp. 13-29.

Ingólfsson, O., Norðdahl, H., 2001. High Relative Sea Level during the Bolling Interstadial in Western Iceland: A Reflection of Ice-Sheet Collapse and Extremely Rapid Glacial Unloading. Arctic, Antarct. Alp. Res. 33, 231. https://doi.org/10.2307/1552224

Ivy-Ochs, S., Synal, H.-A., Roth, C., Schaller, M., 2004. Initial results from isotope dilution for Cl and 36Cl measurements at the PSI/ETH Zurich AMS facility. Nucl. Instruments Methods Phys. Res. Sect. B Beam Interact. with Mater. Atoms 223–224, 623–627. https://doi.org/10.1016/j.nimb.2004.04.115

Janke, J.R., Bellisario, A.C., Ferrando, F.A., 2015. Classification of debris-covered glaciers and rock glaciers in the Andes of central Chile. Geomorphology 241, 98-121. http://dx.doi.org/10.1016/j.geomorph.2015.03.034

Janke, J.R., Regmi, N.R., Giardino, J.R., Vitek, J.D., 2013. 8.17 Rock glaciers. In: Shroder, J. (Ed.), Treatise in Geomorphology, Volume 8. Elsevier, pp. 238-273. https://www.researchgate.net/publication/237102263_Rock_Glacier.

Johnson, P.G., 1980. Rock glaciers: glacial and non-glacial origins. World Glacier Inventory - inventaire mondial des Glaciers. In: (Proceedings of the Riederalp Workshop, September 1978: Actes de l'Atelier de Riederalp, septembre 1978), vol.

126. International Association of Scientific Hydrology, pp. 285e293. http://hydrologie.org/redbooks/a126/iahs_126_0285.pdf.

Jones, D.B., Harrison, S., Anderson, K., Selley, H.L., Wood, J.L., Betts, R.A., 2018. The distribution and hydrological significance of rock glaciers in the Nepalese Himalaya. Glob. Planet. Change 160, 123–142. https://doi.org/10.1016/J.GLOPLACHA.2017.11.005

Jónsson, O., 1976. Berghlaup. Ræktunarfélag Norðurlands, Akureyri.

Kaldal, I., Víkingsson, S. 1990. Early Holocene deglaciation in Central Iceland. Jökull 40, 51-66.

Kellerer-Pirklbauer, A., 2012. The Schmidt-Hammer as a Relative Age Dating Tool for Rock Glacier Surfaces. Quat. Int. 279–280, 239. https://doi.org/10.1016/J.QUAINT.2012.08.546

Kellerer-Pirklbauer, A., Kaufmann, V., 2012. About the relationship between rock glacier velocity and climate parameters in central Austria. Austrian J. Earth Sci. 105, 94–112.

Kellerer-Pirklbauer, A., Lieb, G.K., Avian, M., G., J., 2008. The response of partially debris- covered valley glaciers to climate change: the example of the Pasterze glacier (Austria) in the period 1964 to 2006. Geogr. Ann. Ser. A, Phys. Geogr. 90, 269–285. https://doi.org/10.1111/j.1468-0459.2008.00345.x

Kellerer-Pirklbauer, A., Lieb, G.K., Kaufmann, V., 2017. The Dösen Rock Glacier in Central Austria: A key site for multidisciplinary long-term rock glacier monitoring in the Eastern Alps. Austrian J. Earth Sci. 110. https://doi.org/10.17738/ajes.2017.0013

Kellerer-Pirklbauer, A., Wangensteen, B., Farbrot, H., Etzelmüller, B., 2007. Relative surface age-dating of rock glacier systems near Hólar in Hjaltadalur, northern Iceland. J. Quat. Sci. 23, 137–151. https://doi.org/10.1002/jqs.1117

Kenner, R., 2018. Geomorphological analysis on the interaction of Alpine glaciers and rock glaciers since the Little Ice Age. L. Degrad. Dev. https://doi.org/10.1002/ldr.3238

Kenner, R., Phillips, M., Limpach, P., Beutel, J., Hiller, M., 2018. Monitoring mass movements using georeferenced time-lapse photography: Ritigraben rock glacier, western Swiss Alps. Cold Regions Science and Technology 145, 127–134.

Kirkbride, M.P., 2000. Ice-marginal geomorphology and Holocene expansion of debris-covered Tasman glacier, New Zealand. In: Nakawo, M., Raymond, C.F., Fountain, A. (Eds.), Debris-covered Glaciers, vol. 264. IAHS, pp. 211-217. http://hydrologie.org/redbooks/a264/iahs_264_0211.pdf.

Kirkbride, M.P., 2011. Debris-covered glaciers. In: Singh, V.P., Singh, P., Haritashya, U.K. (Eds.), Encyclopedia of Snow, Ice and Glaciers: Encyclopedia of Earth Series. Springer, Netherlands, pp. 180–182. https://doi.org/10.1007/978-90-481-2642-2_622

Knight, J., Harrison, S., Jones, D.B., 2018. Rock glaciers and the geomorphological evolution of deglacierizing mountains. Geomorphology 311, 127–142. https://doi.org/10.1016/j.geomorph.2018.09.020

Konrad, S.K., Clark, D.C. 1998. Evidence for an Early Neoglacial Glacier Advance from Rock Glaciers and Lake Sediments in the Sierra Nevada, California, U.S.A. Arctic and Alpine Research 30 (3), 272-284. http://www.jstor.org/stable/1551975

Humlum, O., 2000. The geomorphic significance of rock glaciers: estimates of rock glacier debris volumes and headwall recession rates in West Greenland. Geomorphology 35, 41–67. https://doi.org/10.1016/S0169-555X(00)00022-2

Kugelmann, O., 1991. Dating Recent Glacier Advances in the Svarfaðardalur-Skíðadalur Area of Northern Iceland by Means of a New Lichen Curve, in: Maizels, J.K., Caseldine, C. (Eds.), Environmental Change in Iceland: Past and Present. Glaciology and Quaternary Geology, Vol 7. Springer, Dordrecht, pp. 203–217. https://doi.org/10.1007/978-94-011-3150-6_14

Larsen, D.J., Miller, G.H., Geirsdóttir, Á., Ólafsdóttir, S., 2012. Non-linear Holocene climate evolution in the North Atlantic: A high-resolution, multi-proxy record of glacier activity and environmental change from Hvítárvatn, central Iceland. Quat. Sci. Rev. 39, 14–25. https://doi.org/10.1016/j.quascirev.2012.02.006

Leonard, E. M., Laabs, B. J. B., Schweinsberg, A. D., Russell, C. M., Briner, J. P., & Young, N. E. (2017). Deglaciation of the Colorado Rocky Mountains following the Last Glacial Maximum. Cuadernos de Investigación Geográfica, 43(2), 497-526. http://dx.doi.org/10.18172/cig.3234

Li, Y.K., 2018. Determining topographic shielding from digital elevation models for cosmogenic nuclide analysis: a GIS model for discrete sample sites. Journal of Mountain Science 15(5), 939-947. https://doi.org/10.1007/s11629-018-4895-4

Licciardi, J.M., Denoncourt, C.L., Finkel, R.C., 2008. Cosmogenic ^{36}Cl production rates from Ca spallation in Iceland. Earth Planet. Sci. Lett. 267, 365–377. https://doi.org/10.1016/j.epsl.2007.11.036

Licciardi, J.M., Kurz, M.D., Curtice, J.M., 2006. Cosmogenic 3He production rates from Holocene lava flows in Iceland. Earth Planet. Sci. Lett. 246, 251–264. https://doi.org/10.1016/j.epsl.2006.03.016

Licciardi, J.M., Kurz, M.D., Curtice, J.M., 2007. Glacial and volcanic history of Icelandic table mountains from cosmogenic 3He exposure ages. Quat. Sci. Rev. 26, 1529–1546. https://doi.org/10.1016/j.quascirev.2007.02.016

Licciardi, J. M., and Pierce, K. L, 2018. History and dynamics of the Greater Yellowstone Glacial System during the last two glaciations. Quaternary Science Reviews, 200, 1-33. https://doi.org/10.1016/j.quascirev.2018.08.027

Lilleøren, K.S., Etzelmüller, B., Gärtner-Roer, I., Kääb, A., Westermann, S., Gumundsson, Á., 2013. The Distribution, Thermal Characteristics and Dynamics of Permafrost in Tröllaskagi, Northern Iceland, as Inferred from the Distribution of Rock Glaciers and Ice-Cored Moraines. Permafr. Periglac. Process. 24, 322–335. https://doi.org/10.1002/ppp.1792

Lippl, S., Vijay, S., Braun, M., 2018. Automatic delineation of debris-covered glaciers using InSAR coherence derived from X-, C-and L-band radar data: a case study of Yazgyl Glacier. Journal of Glaciology, 1-11. https://doi.org/10.1017/jog.2018.70

Mackay, S.L., Marchant, D.R., 2016. Dating buried glacier ice using cosmogenic 3He in surface clasts: Theory and application to Mullins Glacier, Antarctica. Quat. Sci. Rev. 140, 75-100. https://doi.org/10.1016/j.quascirev.2016.03.013

Marrero, S.M., Phillips, F.M., Caffee, M.W., Gosse, J.C., 2016. CRONUS-Earth cosmogenic 36Cl calibration. Quat. Geochronol. 31, 199–219. https://doi.org/10.1016/j.quageo.2015.10.002

Martin, H.E., Whalley, B., Orr, J., Caseldine, C., 1994. Dating and interpretation of rock glaciers using lichenometry, south Tröllaskagi, North Iceland. Münchener Geogr. Arb. 12, 205–224.

Matthews, J.M., Nesje, A., Linge, H., 2013. Relict talus-foot rock glaciers at Øyberget, upper Ottadalen, Southern Norway: Schmidt hammer exposure ages and palaeoenvironmental implications. Permafr. Periglac. Process. 24 (4), 336-346. http://dx.doi.org/10.1002/ppp.1794.

Mayr, E., Hagg, W., 2019. Debris-Covered Glaciers. In T. Heckmann and D. Morche (eds.), Geomorphology of Proglacial Systems, Geography of the Physical Environment, pp. 59-71. https://doi.org/10.1007/978-3-319-94184-4_4

Mercier, D., 2008. Paraglacial and paraperiglacial landsystems; concepts, temporal scales and spatial distribution. Géomorphologie, Relief, Processus, Environnement 14, 223-233.

Mercier, D., Coquin, J., Feuillet, T., Decaulne, A., Cossart, E., Jónsson, H.P., Sæmundsson, Þ., 2017. Are Icelandic rock-slope failures paraglacial? Age evaluation of seventeen rock-slope failures in the Skagafjörður area, based on geomorphological stacking, radiocarbon dating and tephrochronology. Geomorphology 296, 45–58. https://doi.org/10.1016/j.geomorph.2017.08.011

Mercier, D., Cossart, E., Decaulne, A., Feuillet, T., Jónsson, H.P., Sæmundsson, Þ., 2013. The Höfðahólar rock avalanche (sturzström): chronological constraint of paraglacial landsliding on an Icelandic hillslope. The Holocene 23, 432–446. https://doi.org/10.1177/0959683612463104

Monnier, S., Kinnard, C., 2015. Reconsidering the glacier to rock glacier transformation problem: new insights from the central Andes of Chile. Geomorphology 238, 47-55. http://dx.doi.org/10.1016/j.geomorph.2015.02.025

Moran, A.P., Ivy-Ochs, S., Vockenhuber, C., Kerschner, H., 2016. Rock Glacier development in the Northern Calcareous Alps at the Pleistocene-Holocene boundary. Geomorphology 273, 178-188. https://doi.org/10.1016/j.geomorph.2016.08.017

Norðdahl, H., 1991a. Late Weichselian and early Holocene deglaciation history of Iceland. Jökull 40, 27-50.

Norðdahl, H., 1991b. A review of the glaciation maximum concept and the deglaciation of Eyjafjörður, North Iceland. In: J. Maizels, C. Caseldine (eds.), Environmental Changes in Iceland: Past and Present, Kluwer Academic Publishers, Dordrecht, pp. 31-47.

Norðdahl, H., Einarsson, T., 2001. Concurrent changes of relative sea-level and glacier extent at the Weichselian–Holocene boundary in Berufjörður, Eastern Iceland. Quat. Sci. Rev. 20, 1607–1622. https://doi.org/10.1016/S0277-3791(01)00006-3

Norðdahl, H., Ingólfsson, Ó., 2015. Collapse of the Icelandic ice sheet controlled by sea-level rise? Arktos 1, 13. https://doi.org/10.1007/s41063-015-0020-x

Norðdahl, H., Ingólfsson, O., Pétursson, H.G. Hallsdóttir, M., 2008. Late Weichselian and Holocene environmental history of Iceland. Jökull 58, 343–364.

Norðdahl, H., Pétursson, H. G., 2005. Relative sea level changes in Iceland. New aspects of the Weichselian deglaciation of Iceland. In Caseldine, C., Russel, A.,

Harðardóttir, J., Knudsen, O. (eds.): Iceland - Modern Processes and Past Environments, 25–78. Elsevier, Amsterdam.

Oliva, M., Serrano, E., Gómez-Ortiz, A., González-Amuchástegui, M. J., Nieuwendam, A.; Palacios, D., Pérez-Alberti, A., Pellitero, R., Ruiz-Fernández, J., Valcárcel, M., Vieira, G., Antoniades, D., 2016. Spatial and temporal variability of periglaciation of the Iberian Peninsula. Quaternary Science Reviews 137, 176-199. https://doi.org/10.1016/j.quascirev.2016.02.017

Paasche, Ø., Olaf Dahl, S., Bakke, J., Løvlie, R., Nesje, A., 2007. Cirque glacier activity in arctic Norway during the last deglaciation. Quat. Res. 68, 387–399. https://doi.org/10.1016/J.YQRES.2007.07.006

Palacios, D., Andrés, N., García-Ruiz, J. M., Schimmelpfennig, I., Campos, N., Léanni, L., Aster Team, 2017. Deglaciation in the central Pyrenees during the Pleistocene–Holocene transition: timing and geomorphological significance. Quat. Sci. Rev. 150, 110-129.

Palacios, D., Andrés, N., López-Moreno, J.I., García-Ruiz, J.M., 2015b. Late Pleistocene deglaciation in the upper Gállego valley, central Pyrenees. Quat. Res. 83, 397-414. https://doi.org/10.1016/j.yqres.2015.01.010

Palacios, D., Andrés, N., Marcos, J., Vázquez-Selem, L., 2012. Glacial landforms and their paleoclimatic significance in Sierra de Guadarrama, central Iberian Peninsula. Geomorphology 139-140, 67-78. https://doi.org/10.1016/j.geomorph.2011.10.003

Palacios, D., Gómez-Ortiz, A., Andrés, N., Salvador-Franch, F., Oliva, M., 2016. Timing and new geomorphologic evidence of the last deglaciation stages in Sierra Nevada (southern Spain). Quat. Sci. Rev. 150, 110-129. https://doi.org/10.1016/j.quascirev.2016.08.012

Palacios, D., Gómez-Ortiz, A., Andrés, N., Vázquez-Selem, L., Salvador-Franch, F., Oliva, M., 2015a. Maximum extent of Late Pleistocene glaciers and last deglaciation of La Cerdanya mountains, southeastern Pyrenees. Geomorphology 231, 116-129. https://doi.org/10.1016/j.geomorph.2014.10.037

Patton, H., Hubbard, A., Bradwell, T., Schomacker, A., 2017. The configuration, sensitivity and rapid retreat of the Late Weichselian Icelandic ice sheet. Earth-Science Rev. 166, 223–245. https://doi.org/10.1016/J.EARSCIREV.2017.02.001

Pelto, M., Capps, D., Clague, J.J., Pelto, B., 2013. Rising ELA and expanding proglacial lakes indicate impending rapid retreat of Brady Glacier, Alaska. Hydrol. Process. 27, 3075–3082. https://doi.org/10.1002/hyp.9913.

Pétursson, H.G., Norðdahl, H., Ingólfsson, Ó., 2015. Late Weichselian history of relative sea level changes in Iceland during a collapse and subsequent retreat of marine based ice sheet. Cuad. Investig. Geográfica 41, 261. https://doi.org/10.18172/cig.2741

Phillips, F.M., 2003. Cosmogenic 36Cl ages of Quaternary basalt flows in the Mojave Desert, California, USA. Geomorphology 53, 199–208. http://dx.doi.org/10.1016/S0169-555X(02)00328-8.

Phillips, F. M., 2016. Cosmogenic nuclide data sets from the Sierra Nevada, California, for assessment of nuclide production models: I. Late Pleistocene glacial chronology. Quaternary Geochronology, 35, 119-129. https://doi.org/10.1016/j.quageo.2015.12.003

Potter, N.J., Steig, E.J., Clark, D.H., Speece, M.A., Clark, G.M., Updike, A.B., 1998. Galena Creek rock glacier revisited—new observations on an old controversy.

Geogr. Ann. Ser. A, Phys. Geogr. 80, 251–265. https://doi.org/10.1111/j.0435-3676.1998.00041.x.

Principato, S.M., Geirsdóttir, Á., Jóhannsdóttir, G.E., Andrews, J.T., 2006. Late Quaternary glacial and deglacial history of eastern Vestfirðir, Iceland using cosmogenic isotope (36Cl) exposure ages and marine cores. J. Quat. Sci. 21, 271–285. http://dx.doi.org/10.1002/jqs.978

Rangecroft, S., Harrison, S., Anderson, K., 2015. Rock glaciers as water stores in the Bolivian Andes: an assessment of their hydrological importance. Arctic, Antarctic, and alpine research, 47(1), 89-98. https://doi.org/10.1657/AAAR0014-029

Ribolini, A., Chelli, A., Guglielmin, M., Pappalardo, M., 2007. Relationships between glacier and rock glacier in the Maritime Alps, Schiantala Valley, Italy. Quat. Res. 68, 353–363. https://doi.org/10.1016/j.yqres.2007.08.004

Rodríguez-Rodríguez, L., Jiménez-Sánchez, M., Domínguez-Cuesta, M.J., Rinterknecht, V., Pallàs, R., Aster Team, 2017. Timing of last deglaciation in the Cantabrian Mountains (Iberian Peninsula; North Atlantic region) based on in situ-produced 10Be exposure dating. Quat. Sci. Rev. 171, 166-181. https://doi.org/10.1016/j.quascirev.2017.07.012

Rosenwinkel, S., Korup, O., Landgraf, A., Dzhumabaeva, A., 2015. Limits to lichenometry. Quat. Sci. Rev. 129, 229-238. http://dx.doi.org/10.1016/j.quascirev.2015.10.031.

Rundgren, M., 1995. Biostratigraphic Evidence of the Allerød-Younger Dryas-Preboreal Oscillation in Northern Iceland. Quat. Res. 44, 405–416. https://doi.org/10.1006/QRES.1995.1085

Rundgren, M., Ingólfsson, Ó. 1999. Plant survival in Iceland during periods of glaciations. Journal of Biogeography 26, 387-396.

Sæmundsson, K., Kristjansson, L., McDougall, I., Watkins, N.D., 1980. K-Ar dating, geological and paleomagnetic study of a 5-km lava succession in northern Iceland. J. Geophys. Res. Solid Earth 85, 3628–3646. https://doi.org/10.1029/JB085iB07p03628

Scapozza, C., Lambiel, C., Bozzini, C., Mari, S., Conedera, M., 2014. Assessing the rock glacier kinematics on three different timescales: A case study from the southern Swiss Alps. Earth Surf. Process. Landforms 39, 2056–2069. https://doi.org/10.1002/esp.3599

Schimmelpfennig, I., 2009. Cosmogenic 36Cl in Ca and K rich minerals: analytical developments, production rate calibrations and cross calibration with 3He and 21Ne. Doctor Thesis, Universite Paul Cezanne Aix-Marseille III, CEREGE, 324 pp.

Schimmelpfennig, I., Benedetti, L., Finkel, R., Pik, R., Blard, P.H., Bourlès, D., Burnard, P., Williams, A., 2009. Sources of in-situ36Cl in basaltic rocks. Implications for calibration of production rates. Quat. Geochronol. 4, 441–461. https://doi.org/10.1016/j.quageo.2009.06.003

Schimmelpfennig, I., Benedetti, L., Garreta, V., Pik, R., Blard, P.H., Burnard, P., Bourlès, D., Finkel, R., Ammon, K., Dunai, T., 2011. Calibration of cosmogenic 36Cl production rates from Ca and K spallation in lava flows from Mt. Etna (38°N, Italy) and Payun Matru (36°S, Argentina). Geochim. Cosmochim. Acta 75, 2611–2632. https://doi.org/10.1016/j.gca.2011.02.013

Schimmelpfennig, I., Schaefer, J.M., Putnam, A.E., Koffman, T., Benedetti, L., Ivy-Ochs, S., Team, A., Schlüchter, C., 2014. 36 Cl production rate from K-spallation in the European Alps (Chironico landslide, Switzerland). J. Quat. Sci. 29, 407–413. https://doi.org/10.1002/jqs.2720

Schomacker, A., Brynjólfsson, S., Andreassen, J.M., Gudmundsdóttir, E.R., Olsen, J., Odgaard, B. V., Håkansson, L., Ingólfsson, Ó., Larsen, N.K., 2016. The Drangajökull ice cap, northwest Iceland, persisted into the early-mid Holocene. Quat. Sci. Rev. 148, 68–84. https://doi.org/10.1016/J.QUASCIREV.2016.07.007

Sigurðsson, O., Williams, R.S., 2008. Geographic names of Icelandic glaciers: historic and modern. US Geological Survey Professional Paper 1746.

Stone, J.O., 2000. Air pressure and cosmogenic isotope production. J. Geophys. Res. Solid Earth 105, 23753–23759. https://doi.org/10.1029/2000JB900181

Stone, J.O., Fifielde, K., Vasconcelos, P., 2005. Terrestrial chlorine-36 production from spallation of iron, in: Abstract of 10th International Conference on Accelerator Mass Spectrometry. Berkeley, CA.

Stötter, J., Wastl, M., Caseldine, C., Häberle, T., 1999. Holocene palaeoclimatic reconstruction in northern Iceland: Approaches and results. Quat. Sci. Rev. 18, 457–474. https://doi.org/10.1016/S0277-3791(98)00029-8

Swanson, T.W., Caffee, M.L., 2001. Determination of 36Cl production rates derived from the well-dated deglaciation surfaces of Whidbey and Fidalgo Islands, Washington. Quat. Res. 56, 366–382. https://doi.org/10.1006/qres.2001.2278

Sæmundsson, Þ., Morino, C., Helgason, J.K., Conway, S.J. & Pétursson, H.G. 2018: The triggering factors of the Móafellshyrna debris slide in northern Iceland: intense

precipitation, earthquake activity and thawing of mountain permafrost. Science of the Total Environment 621 (2018) 1163–1175.

Tanarro, L.M., Palacios, D., Andrés, N., Fernández-Fernández, J.M., Zamorano, J.J., Sæmundsson, Þ., Brynjólfsson, S., 2019. Unchanged surface morphology in debris-covered glaciers and rock glaciers in Tröllaskagi peninsula (northern Iceland). Sci. Total Environ. 648, 218–235. https://doi.org/10.1016/j.scitotenv.2018.07.460

Tanarro, L.M., Palacios, D., Zamorano, J.J., Andrés, N., 2018. Proposal for geomorphological mapping of debris-covered and rock glaciers and its application to Tröllaskagi Peninsula (Northern Iceland). J. Maps 14, 692–703. https://doi.org/10.1080/17445647.2018.1539417

Vázquez-Selem, L., & Lachniet, M. S., 2017. The deglaciation of the mountains of Mexico and Central America. Cuadernos de Investigación Geográfica, 43(2), 553-570. http://dx.doi.org/10.18172/cig.3238

Wangensteen, B., Gudmundsson, Á., Eiken, T., Kääb, A., Farbrot, H., Etzelmüller, B., 2006. Surface displacements and surface age estimates for creeping slope landforms in Northern and Eastern Iceland using digital photogrammetry. Geomorphology 80, 59–79. https://doi.org/10.1016/j.geomorph.2006.01.034

Wastl, M., Stotter, J., Caseldine, C., 2001. Reconstruction of Holocene Variations of the Upper Limit of Tree or Shrub Birch Growth in Northern Iceland Based on Evidence from Vesturardalur-Skíðadalur, Tröllaskagi. Arctic, Antarct. Alp. Res. 33, 191. https://doi.org/10.2307/1552220

Whalley, W.B., Douglas, G.R., Jonsson, A., 1983. The Magnitude and Frequency of Large Rockslides in Iceland in the Postglacial. Geogr. Ann. Ser. A, Phys. Geogr. 65, 99–110. https://doi.org/10.2307/520724

Whalley, W.B., Hamilton, S., Palmer, C., Gordon, J., Martin, H.E., 1995. The dynamics of rock glaciers: data from Tröllaskagi, North Iceland. In: Slaymaker, O. (Ed.), Steepland Geomorphology. John Wiley & Sons, pp. 129–145.

Whalley, W.B., Palmer, C.F., Hamilton, S.J., Martin, H.E., 1995. An Assessment of Rock Glacier Sliding Using Seventeen Years of Velocity Data: Nautárdalur Rock Glacier, North Iceland. Arct. Alp. Res. 27, 345–351. https://doi.org/10.2307/1552027

Winkler, S., Lambiel, C., 2018. Age constraints of rock glaciers in the Southern Alps/New Zealand – Exploring their palaeoclimatic potential. Holocene 28, 778–790. https://doi.org/10.1177/0959683618756802

Wirz, V., Gruber, S., Purves, R.S., Beutel, J., Gärtner-Roer, I., Gubler, S., Vieli, A., 2016. Short-term velocity variations at three rock glaciers and their relationship with meteorological conditions. Earth Surf. Dyn. 4, 103–123. https://doi.org/10.5194/esurf-4-103-2016

Xiao, X., Zhao, M., Knudsen, K.L., Sha, L., Eiríksson, J., Gudmundsdóttir, E., Jiang, H., Guo, Z., 2017. Deglacial and Holocene sea–ice variability north of Iceland and response to ocean circulation changes. Earth Planet. Sci. Lett. 472, 14–24. https://doi.org/10.1016/J.EPSL.2017.05.006

Zreda, M., England, J., Phillips, F., Elmore, D., Sharma, P., 1999. Unblocking of the Nares Strait by Greenland and Ellesmere icesheet retreat 10,000 years ago. Nature 398, 139–142. http://dx.doi.org/10.1038/18197

Figure captions

Figure 1. Location of the study area in central north Iceland (A) the Tröllaskagi peninsula (B) and glaciers and debris-covered glaciers under study (C). The red boxes show the extent of the aerial photos and maps corresponding to the Figures 2, 3 and 6. This figure is available in color in the online version.

Figure 2. View of the Fremri-Grjótárdalur rock glacier complex and spatial distribution of ^{36}Cl CRE samples and photogrammetry-tracked boulders. Stable area refers where it is known that the boulder movement of less than 0.16 m yr^{-1}. The red dashed line indicates the edge between the relict and active rock glaciers. This figure is available in color in the online version.

Figure 3. Overhead view of the Hofsjökull glacier complex and spatial distribution of ^{36}Cl CRE samples and photogrammetry-tracked boulders. Panel A shows the whole glacier complex (debris-free and debris-covered sectors). Panel B is a zoom of the frontal area. Stable area refers where it is known that the boulder movement is less than 0.37 m yr^{-1}. This figure is available in color in the online version.

Figure 4. View of the Héðinsdalsjökull glacier complex and spatial distribution of ^{36}Cl CRE samples and photogrammetry-tracked boulders. Panel A shows the whole glacier complex (debris-free and fossil/active debris-covered sectors). Panel B is a zoom of the frontal area. The red dashed line in panel A indicates the edge between the collapsed and active debris-covered glaciers. This figure is available in color in the online version.

Figure 5. A) Location of sample ELLID-1 viewed from the west, on the northern side of the Hóladalur valley. Hólajökull and Fremri-Grjótárdalur cirques at the bottom. B) Location of sample ELLID-2 viewed from the east. The Skagafjörður fjord can be seen

at the bottom. Ages results from samples: ELLID-1: 16.3±1.2 ka; ELLID-2:16.3±0.9 ka. This figure is available in color in the online version.

Figure 6. Location of samples describing the deglaciation pattern of the study area. The red box corresponds to the extent of the Figure 2. This figure is available in color in the online version.

Figure 7. Photos of the Fremri-Grjótárdalur rock glacier complex. A) View of the rock glacier complex from the summit area to the north. B) Sample FDG-1 in the relict rock glacier. C) Sample FDG-11 in the lateral moraine located in front of the rock glaciers. D) View of the rock glacier complex from the eastern sector of the cirque. This figure is available in color in the online version.

Figure 8. Idealized longitudinal profile of the Fremri-Grjótárdalur rock glaciers and the relative position of the ^{36}Cl CRE samples. The inner structure is speculative. This figure is available in color in the online version.

Figure 9. Field photos of Hóladalur cirque. A) Oblique view of the Hóladalsjökull debris-covered glacier from the western summit area. B) Sample HOL-1 in a moraine in front of the debris-covered glacier. C) Close up view of the debris-covered glacier snout. This figure is available in color in the online version.

Figure 10. Field photos of Hofsjökull cirque. A) Oblique view of the Hofsjökull debris-covered glacier from the southern summit area. B) Close up view of the debris-covered glacier snout. C) Sample HOFS-1 on a crest located in the frontal area of the debris-covered glacier. This figure is available in colour in the online version.

Figure 11. Field photos of Héðinsdalsjökull glacier. A) Oblique view of the Héðinsdalsjökull debris-covered glacier from the south. B) Middle sector of the debris-covered glacier with internal ice. C) Snout of the debris-covered glacier in the current

fossil stage. D) Sample HEDIN-2 on a crest in the frontal area of the debris-covered glacier. E) Sample HEDIN-1 on the crest in the frontal area of the debris-covered glacier. This figure is available in color in the online version.

Figure 12. Idealized model about the evolution of glaciers in the Tröllaskagi mountains according to the CRE dating results. A) The main valleys of the interior of Tröllaskagi were covered with ice before 16 ka, feeding the glacier outlet of Skagafjörður. B) Around 16 ka a series begins of rapid, intense, glaciological and geomorphological processes; the sequence can be determined, but the uncertainty of the CRE results prevents an accurate timing of each specific moment. Deglaciation begins around 16 ka and glaciers in the interior of Tröllaskagi become disconnected from the Skagafjörður glacier outlet. C) Subsequently, the main valleys are deglaciated with a small advance inside the cirques around 11ka. D) The first rock glacier generation forms around 11-10 ka. E) The glacier fronts rapidly become inactive around 10 ka. F) After 10 ka, a new generation of rock glaciers forms and their dynamics begin to stabilize 5-3 ka according to their altitude. Note that the debris mantle of the stage D contributed to form the deposits of the relict rock glacier of the following stage E.

Table captions

Table 1. Inventory of the photogrammetry-tracked boulders surveyed in the different geomorphological units their mobility measurements for the 1980-1994 period. Note that the low mobility figures pose the sampled boulders as highly reliable.

Table 2. Geographic sample locations, topographic shielding factor, sample thickness and distance from headwall.

Table 3. Concentrations of the ^{36}Cl target elements Ca, K, Ti and Fe Ca, K, Ti and Fe, determined in splits taken after the chemical pre-treatment (acid etching).

Table 4. Chemical composition of the bulk rock samples before chemical treatment.

Table 5. ^{36}Cl CRE dating results. The numbers in italics correspond to the internal (analytical) uncertainty at one standard level.

Table 1. Inventory of the photogrammetry-tracked boulders surveyed in the different geomorphological units their mobility measurements for the 1980-1994 period. Note that the low mobility figures pose the sampled boulders as highly reliable.

CRE sample	Analized boulders	Year 1980			Year 1994			1980-1994 period	
		X (m)	Y (m)	Elevation (m a.s.l.)	X (m)	Y (m)	Elevation (m a.s.l.)	Horizontal displacement	
								Absolute (m 14 yr^{-1})	Velocity (m yr^{-1})
HOL-1	B-1	501384.27	581422.77	835.36	501384.99	581422.70	835.32	0.723	0.052
HOL-2	B-2	501393.24	581350.79	839.98	501392.94	581350.62	840.04	0.345	0.025
FDG-11	B-4	499246.73	580783.27	897.57	499247.03	580781.79	897.53	1.510	0.108
	B-5	499248.00	580769.41	898.00	499247.80	580768.72	897.93	0.718	0.051
	B-6	499266.84	580740.85	899.42	499267.27	580740.50	899.74	0.554	0.040
FDG-1, FDG-2	B-7	498805.31	580940.54	871.31	498804.97	580940.22	871.04	0.467	0.033
	B-8	498828.64	580944.99	866.63	498828.92	580944.85	866.20	0.313	0.022
	B-9	498871.17	580933.82	867.89	498871.83	580933.79	867.78	0.661	0.047
FGD-1B, FGD-2B, FGD-3B	B-10	499163.16	580369.13	950.27	499161.8	580370.94	950.20	2.264	0.162
	B-11	499153.50	580345.39	951.61	499153.30	580347.20	951.57	1.821	0.130
	B-12	499172.04	580338.82	953.45	499171.96	580340.40	953.62	1.582	0.113
	B-13	499221.77	580333.74	952.24	499221.59	580334.79	952.16	1.065	0.076
	B-14	499153.33	580314.13	956.72	499152.87	580315.89	956.53	1.819	0.130
FGD-4B, FGD-5B	B-15	499645.82	580131.39	989.73	499645.73	580131.51	989.76	0.150	0.011
	B-16	499659.70	580127.30	993.74	499659.43	580127.46	993.38	0.314	0.022
	B-17	499651.98	580097.27	992.21	499651.94	580097.29	992.00	0.045	0.003
HOFS-1, HOFS-2, HOFS-3	B-18	502428.88	575959.77	887.63	502424.46	575959.28	887.04	4.447	0.318
	B-19	502393.88	575939.80	884.95	502390.67	575943.19	883.69	4.669	0.333
	B-20	502400.52	575931.57	887.51	502396.74	575934.19	886.48	4.599	0.329
	B-21	502411.46	575920.45	891.44	502407.88	575923.78	890.89	4.889	0.349
	B-22	502413.24	575917.63	892.38	502409.12	575920.74	891.60	5.162	0.369
	B-23	502416.01	575675.23	926.16	502412.97	575677.98	925.85	4.099	0.293
	B-24	502382.18	575667.46	923.25	502379.86	575669.72	923.06	3.239	0.231

B-25	502408.02	575627.08	933.75	502406.13	575628.55	933.42	2.394	0.171	-
B-26	502400.35	575616.67	934.97	502398.34	575618.54	934.54	2.745	0.196	-
B-27	502425.77	575603.09	940.43	502423.72	575604.54	940.39	2.511	0.179	-

Table 2. Geographic sample locations, topographic shielding factor, sample thickness and distance from headwall.

ample type	Latitude (ºN)	Longitude (ºW)	Elevation (m a.s.l.)	Shielding factor	Thickness (cm)
ge Elliði					
olished bedrock	65.7580	19.0848	597	0.9986	2.0
olished bedrock	65.7579	19.0854	597	0.9994	3.5
Hóladalur					
Moraine boulder	65.7303	18.9698	833	0.9629	3.0
Moraine boulder	65.7297	18.9696	841	0.9931	3.0
rock glacier complex					
ock glacier (inactive) boulder	65.7259	19.0245	869	0.8889	4.0
ock glacier (inactive) boulder	65.8003	19.0200	874	0.9765	4.5
Moraine boulder	65.7242	19.0159	912	0.9843	5.0
ock glacier (active) boulder	65.7207	19.0172	960	0.9932	2.0
ock glacier (active) boulder	65.7209	19.0186	960	0.9741	4.0
ock glacier (active) boulder	65.7205	19.0186	966	0.9929	3.5
ock glacier (inactive) boulder	65.7184	19.0079	1005	0.9841	3.5
ock glacier (inactive) boulder	65.7187	19.0073	1030	0.9880	4.0
ered glacier					
ebris-covered glacier (active) boulder	65.6812	18.9481	893	0.9758	2.5
ebris-covered glacier (active) boulder	65.6811	18.9478	894	0.9557	4.0
ebris-covered glacier (active) boulder	65.6811	18.9479	903	0.9856	3.5
is-covered glacier					
Moraine boulder	65.6454	18.9292	640	0.9758	3.5
Moraine boulder	65.6455	18.9272	660	0.9764	2.0
Moraine boulder	65.6455	18.9278	653	0.9775	2.5

Table 3. Concentrations of the ^{36}Cl target elements Ca, K, Ti and Fe Ca, K, Ti and Fe, determined in splits taken after the chemical pre-treatment (acid etching).

Sample name	CaO (%)	K_2O (%)	TiO_2 (%)	Fe_2O_3 (%)
Glacially polished ridge Elliði				
ELLID-1	7.20 ± 0.14	0.14 ± 0.02	6.96 ± 0.35	24.28 ± 0.49
ELLID-2	7.01 ± 0.14	0.12 ± 0.02	7.18 ± 0.36	25.12 ± 0.50
Moraine boulders of Hóladalur				
HOL-1	12.05 ± 0.24	0.29 ± 0.04	2.53 ± 0.13	13.16 ± 0.26
HOL-2	11.07 ± 0.22	0.35 ± 0.05	2.93 ± 0.15	14.13 ± 0.28
Fremri-Grjótárdalur rock glacier complex				
FGD-1	11.01 ± 0.22	0.28 ± 0.04	2.66 ± 0.13	14.07 ± 0.28
FGD-2	11.57 ± 0.23	0.33 ± 0.05	2.52 ± 0.13	12.79 ± 0.26
FGD-11	10.92 ± 0.22	0.28 ± 0.04	2.59 ± 0.13	13.70 ± 0.27
FGD-1B	11.37 ± 0.23	0.33 ± 0.05	3.15 ± 0.16	12.68 ± 0.25
FGD-2B	11.73 ± 0.23	0.31 ± 0.05	2.80 ± 0.14	10.60 ± 0.21
FGD-3B	9.88 ± 0.20	0.31 ± 0.05	4.06 ± 0.20	16.71 ± 0.33
FGD-4B	8.59 ± 0.17	0.40 ± 0.06	4.55 ± 0.23	19.70 ± 0.39
FGD-5B	8.96 ± 0.18	0.29 ± 0.04	4.75 ± 0.24	20.58 ± 0.41
Hofsjökull debris-covered glacier				
HOFS-1	9.91 ± 0.20	0.39 ± 0.06	3.54 ± 0.18	17.06 ± 0.34
HOFS-2	9.66 ± 0.19	0.39 ± 0.06	4.50 ± 0.22	18.43 ± 0.37
HOFS-3	9.63 ± 0.19	0.44 ± 0.07	4.37 ± 0.22	18.07 ± 0.36
Héðinsdalsjökull debris-covered glacier				
HEDIN-1	10.28 ± 0.21	0.18 ± 0.03	3.70 ± 0.18	16.91 ± 0.34
HEDIN-2	7.87 ± 0.16	0.80 ± 0.04	2.65 ± 0.13	13.36 ± 0.27
HEDIN-3	8.06 ± 0.16	0.76 ± 0.04	3.05 ± 0.15	14.50 ± 0.29

Table 4. Chemical composition of the bulk rock samples before chemical treatment.

Sample name	CaO (%)	K_2O (%)	TiO_2 (%)	Fe_2O_3 (%)	SiO_2 (%)	Na_2O (%)	MgO (%)	Al_2O_3 (%)	MnO (%)	P_2O_5 (%)	Li (ppm)	B (p
Glacially polished ridge Elliði												
ELLID-1	8.568	0.179	4.753	18.215	44.950	2.161	7.475	12.416	0.228	0.20	4.4	2
Fremri-Grjótárdalur rock glacier complex												
FGD-1B	11.738	0.356	2.590	13.300	47.670	2.395	6.702	13.844	0.194	0.24	4.3	<
FGD-4B	9.580	0.465	3.529	16.270	47.200	2.808	5.223	12.798	0.239	0.34	6.1	<
Hofsjökull debris-covered glacier												
HOFS-1	9.345	0.359	4.267	18.150	48.770	2.225	5.772	10.288	0.250	< L.D	5.4	<
Héðinsdalsjökull debris-covered glacier												
HEDIN-1	10.773	0.262	2.880	14.920	47.290	2.282	6.423	12.918	0.213	0.24	4.4	<

Table 5. ^{36}Cl CRE dating results. The numbers in italics correspond to the internal (analytical) uncertainty at one standard level.

Sample name	Sample weight (g)	Mass of Cl in spike (mg)	$^{35}Cl/^{37}Cl$	$^{36}Cl/^{35}Cl$ (10^{-14})	[Cl] in sample (ppm)	[^{36}Cl] (10^4 aton
Glacially polished ridge Elliði						
ELLID-1	28.88	1.864	64.854 ± 0.615	11.051 ± 0.438	3.5	12.438 ± 0.516
ELLID-2	27.69	1.928	86.476 ± 0.876	10.014 ± 0.437	2.6	11.977 ± 0.547
Moraine boulders of Hóladalur						
HOL-1	30.41	1.012	10.718 ± 0.037	17.257 ± 0. 435	15.6	15.060 ± 0.384
HOL-2	30.89	0.992	9.528 ± 0.066	15.669 ± 0.364	18.3	14.055 ± 0.336
Fremri-Grjótárdalur rock glacier complex						
FGD-1	31.96	1.018	7.805 ± 0.131	13.071 ± 0.399	25.7	13.311 ± 0.444
FGD-2	30.2	0.985	6.026 ± 0.035	13.066 ± 0.395	43.9	17.536 ± 0.547
FGD-11	30.69	1.000	9.585 ± 0.096	17.206 ± 0.568	18.4	15.604 ± 0.525
FGD-1B	70.54	1.883	6.135 ± 0.648	48.960 ± 0.269	36.7	4.304 ± 0.287
FGD-2B	70.34	1.880	5.649 ± 0.646	83.750 ± 0.343	43.8	8.330 ± 0.444
FGD-3B	67.66	1.882	5.888 ± 0.568	10.512 ± 0.412	41.6	10.414 ± 0.521
FGD-4B	26.52	1.851	14.293 ± 0.150	87.158 ± 0.394	25.1	12.908 ± 0.627
FGD-5B	25.78	1.870	11.531 ± 0.115	86.801 ± 0.361	35	14.353 ± 0.655
Hofsjökull debris-covered glacier						
HOFS-1	84.09	1.822	4.289 ± 0.532	68.219 ± 0.356	77.4	9.128 ± 0.670
HOFS-2	85.46	1.832	5.189 ± 0.100	89.175 ± 0.466	43.0	8.026 ± 0.552
HOFS-3	86.23	1.819	4.374 ± 0.671	90.595 ± 0.430	70.2	11.279 ± 0.809
Héðinsdalsjökull debris-covered glacier						
HEDIN-1	67.56	1.878	8.846 ± 0.853	45.314 ± 0.258	19.9	3.167 ± 0.202

HEDIN-2	64.38	1.875	4.706 ± 0.454	25.226 ± 0.165	76.5	3.571 ± 0.286
HEDIN-3	63.98	1.893	4.717 ± 0.438	22.065 ± 0.157	77.1	3.136 ± 0.269
Blanks [a]					*Total atoms Cl* (10^{17})	*Total atoms* ^{36}C (10^{4})
BK-1		1.800	297.029 ± 11.372	0.545 ± 0.097	2.941 ± 0.220	16.981 ± 3.034
BK-2		1.884	356.675 ± 7.637	0.575 ± 0.135	2.313 ± 0.139	18.738 ± 4.384
BK-3		1.888	328.059 ± 2.892	0.359 ± 0.069	2.650 ± 0.136	11.725 ± 2.249
Cblk3125-1		1.897	98.243 ± 1.536	14.248 ± 0.301		
Cblk3125-2		1.859	85.103 ± 0.398	2.228 ± 0.175		

[a] BK-1 was processed with samples HOFS-1, HOFS-2 and HOFS-3; BK-2 was processed with samples FGD-1B, FGD-2B and FGD-3B; BK-3 was processed with samples ELLID-1, ELLID-2, HEDIN-1, HEDIN-2, HEDIN-3, FGD-4B and FGD-5B. Cblk3125-1 and Cblk3125-2 were processed.

Declaration of interests

☒ The authors declare that they have no known competing financial interests or personal relationships that could have appeared to influence the work reported in this paper.

☐The authors declare the following financial interests/personal relationships which may be considered as potential competing interests:

Graphical abstract

Highlights

A novel cosmogenic dating to debris-covered and rock glaciers.

Debris-covered and rock glaciers were formed shortly after deglaciation at 11 ka.

They could have lost the mobility during Holocene Thermal Maximum.

They remain with stagnant ice because they are above the level of permafrost.

Inherent interest in applying cosmogenic dating methods to these formations.

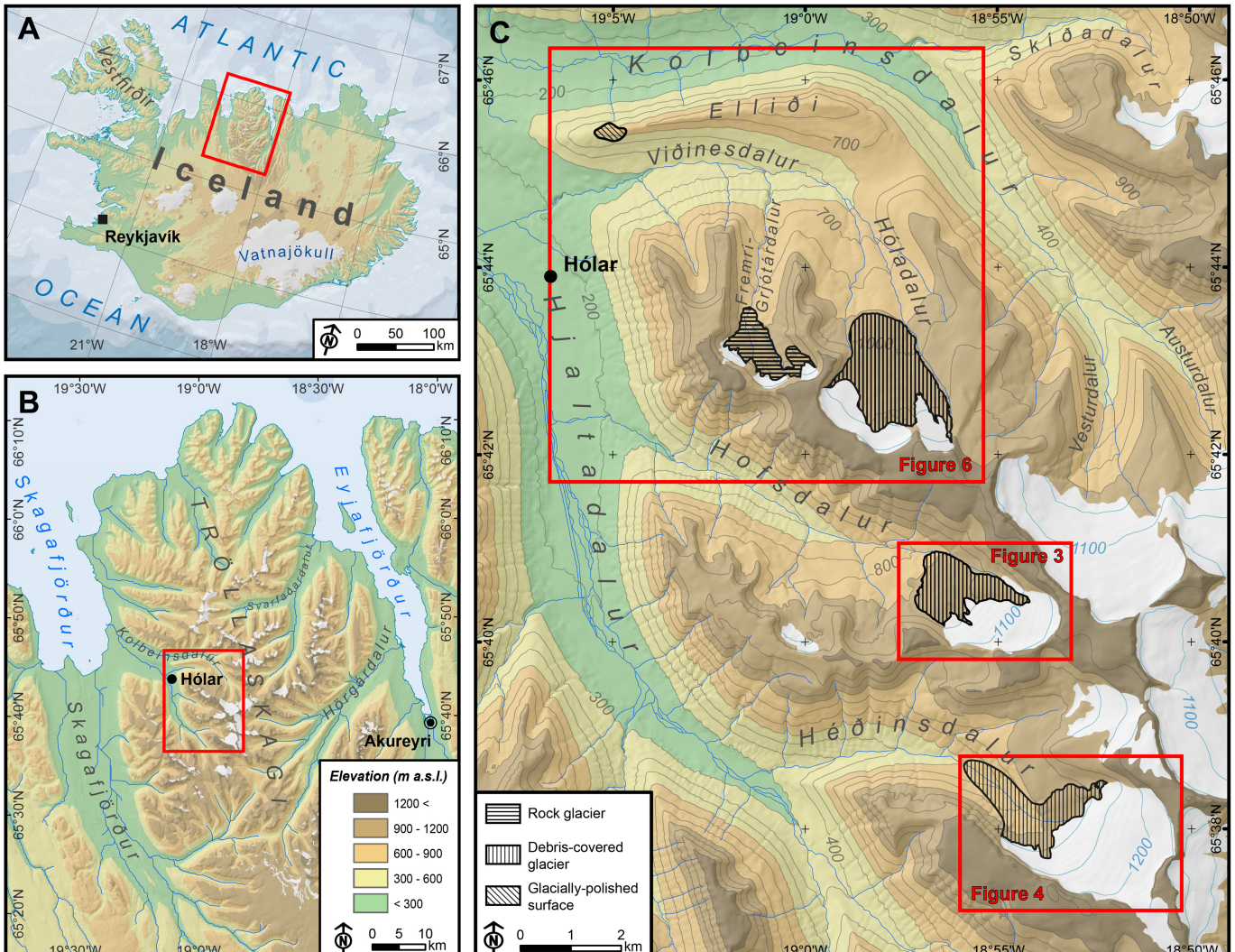
A
ATLANTIC
OCEAN
Iceland
Reykjavík
Vatnajökull
Vestfirðir
21°W
18°W
67°N
66°N
65°N
0 50 100 km
B
19°30'W
19°0'W
18°30'W
18°0'W
66°10'N
66°0'N
65°50'N
65°40'N
65°30'N
65°20'N
Skagafjörður
Eyjafjörður
TRÖLLASKAGI
Svartárdalur
Kolbeinsdalur
Hólar
Hörgárdalur
Skagafjörður
Akureyri
Elevation (m a.s.l.)
1200 <
900 - 1200
600 - 900
300 - 600
< 300
0 5 10 km
C
19°5'W
19°0'W
18°55'W
18°50'W
65°46'N
65°44'N
65°42'N
65°40'N
65°38'N
Kolbeinsdalur
Elliði
Viðinesdalur
Skíðadalur
Hólar
Hjaltadalur
Fremri-Gjástaðadalur
Hóladalur
Hörsdalur
Vesturdalur
Austurdalur
Héðinsdalur
Figure 6
Figure 3
Figure 4
Rock glacier
Debris-covered glacier
Glacially-polished surface
0 1 2 km

Figure 1

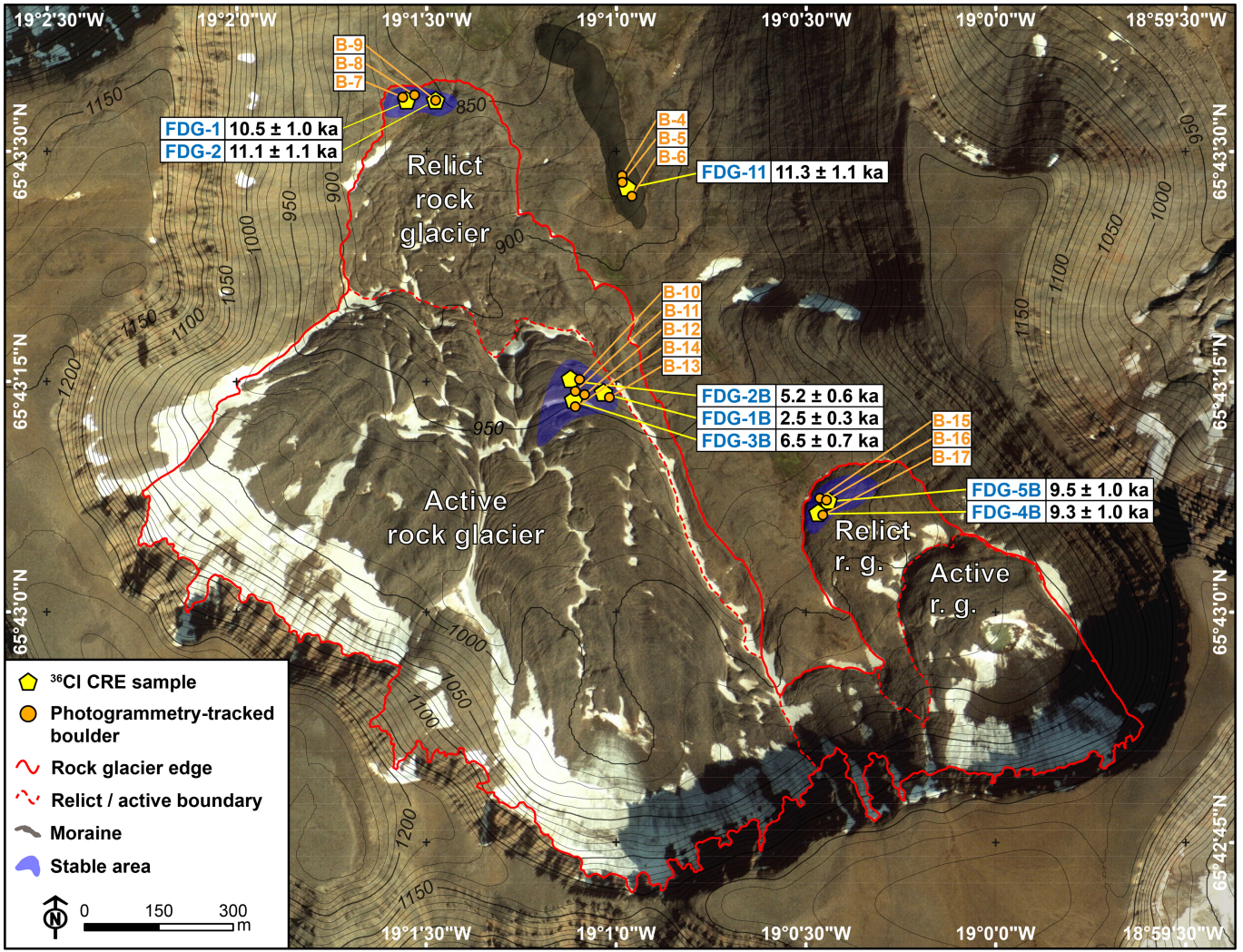
19°2'30"W
19°2'0"W
19°1'30"W
19°1'0"W
19°0'30"W
19°0'0"W
18°59'30"W
65°43'30"N
65°43'15"N
65°43'0"N
65°42'45"N
B-9
B-8
B-7
FDG-1 10.5 ± 1.0 ka
FDG-2 11.1 ± 1.1 ka
Relict rock glacier
B-4
B-5
B-6
FDG-11 11.3 ± 1.1 ka
B-10
B-11
B-12
B-14
B-13
FDG-2B 5.2 ± 0.6 ka
FDG-1B 2.5 ± 0.3 ka
FDG-3B 6.5 ± 0.7 ka
Active rock glacier
B-15
B-16
B-17
FDG-5B 9.5 ± 1.0 ka
FDG-4B 9.3 ± 1.0 ka
Relict r. g.
Active r. g.
850
900
950
1000
1050
1100
1150
1200
36Cl CRE sample
Photogrammetry-tracked boulder
Rock glacier edge
Relict / active boundary
Moraine
Stable area
N
0
150
300
m

Figure 2

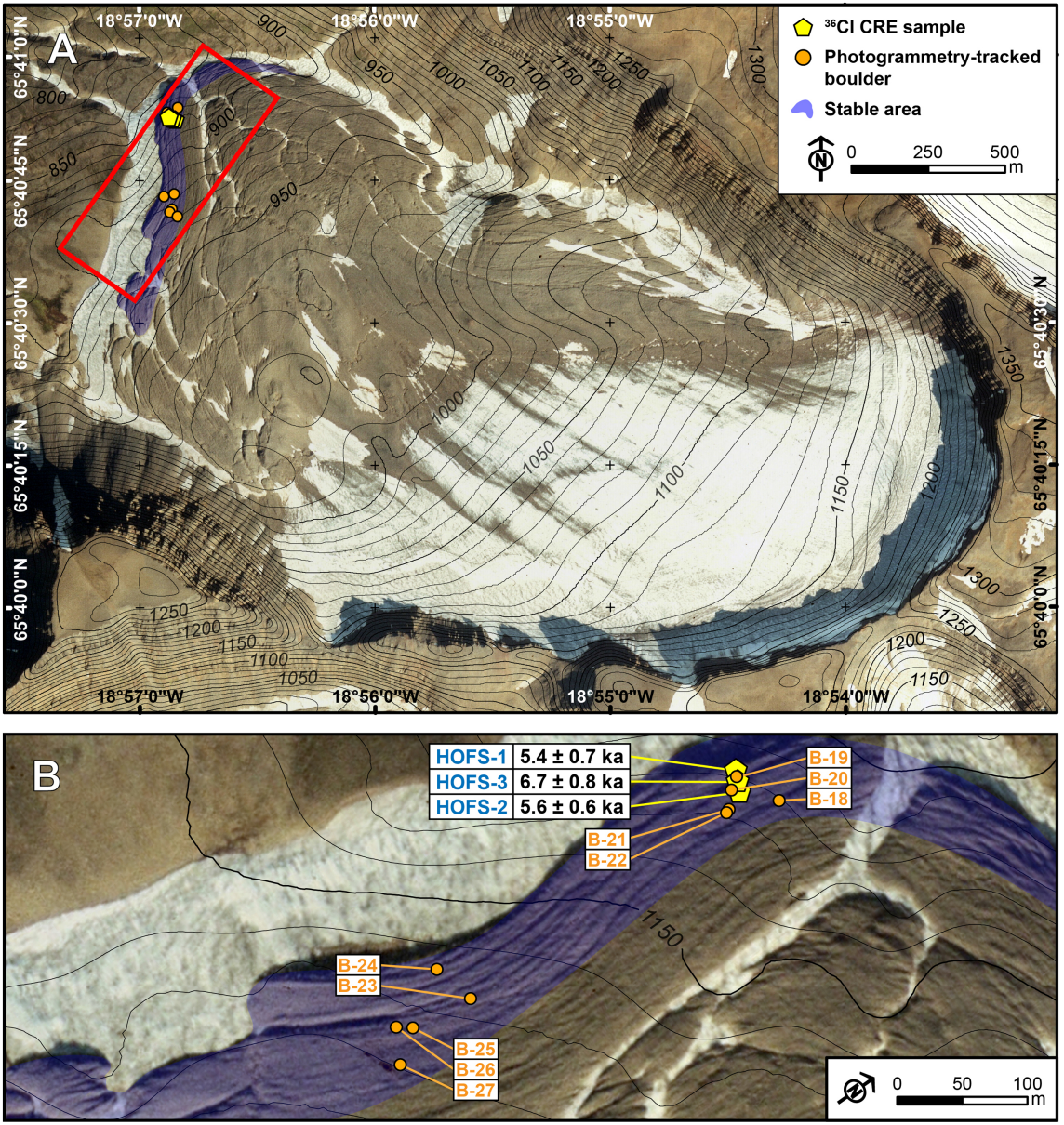
A
B
36Cl CRE sample
Photogrammetry-tracked boulder
Stable area
0 250 500 m
0 50 100 m
18°57'0"W
18°56'0"W
18°55'0"W
18°54'0"W
65°41'0"N
65°40'45"N
65°40'30"N
65°40'15"N
65°40'0"N
HOFS-1 5.4 ± 0.7 ka
HOFS-3 6.7 ± 0.8 ka
HOFS-2 5.6 ± 0.6 ka
B-18
B-19
B-20
B-21
B-22
B-23
B-24
B-25
B-26
B-27

Figure 3

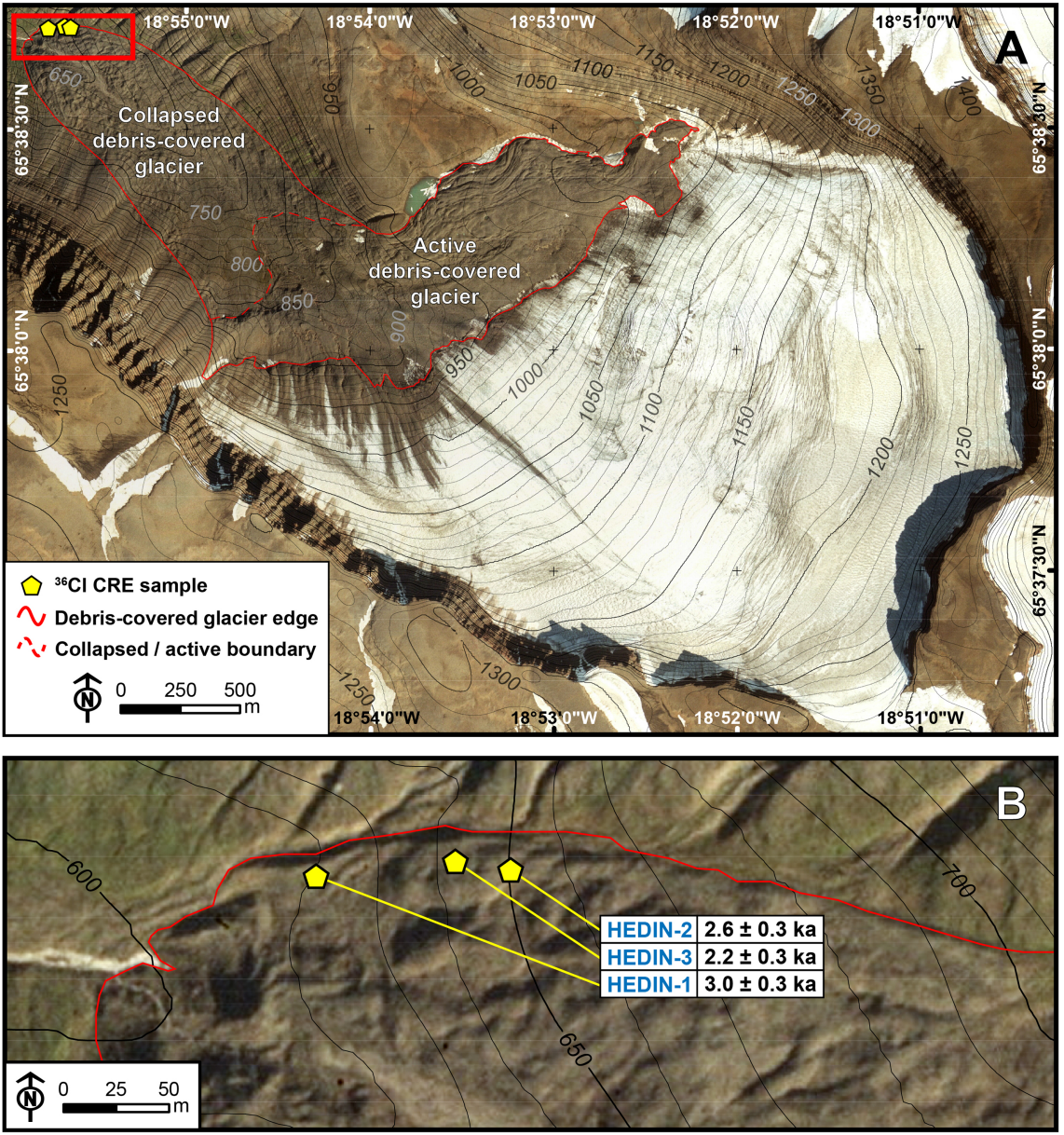
A
18°55'0"W
18°54'0"W
18°53'0"W
18°52'0"W
18°51'0"W
65°38'30"N
65°38'0"N
65°37'30"N
Collapsed debris-covered glacier
Active debris-covered glacier
36Cl CRE sample
Debris-covered glacier edge
Collapsed / active boundary
0 250 500 m
B
HEDIN-2 2.6 ± 0.3 ka
HEDIN-3 2.2 ± 0.3 ka
HEDIN-1 3.0 ± 0.3 ka
0 25 50 m

Figure 4

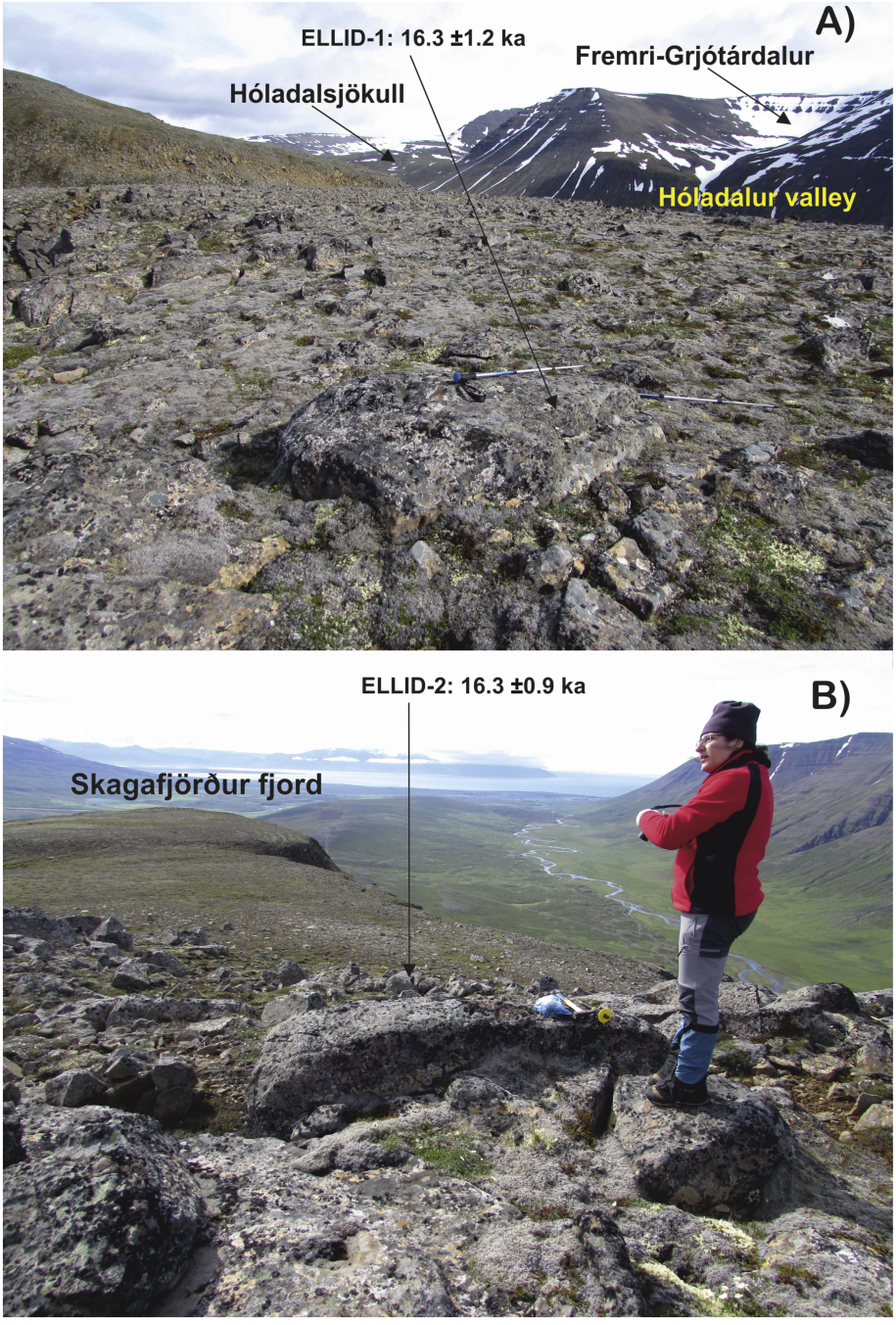
A)
ELLID-1: 16.3 ±1.2 ka
Fremri-Grjótárdalur
Hóladalsjökull
Hóladalur valley
B)
ELLID-2: 16.3 ±0.9 ka
Skagafjörður fjord

Figure 5

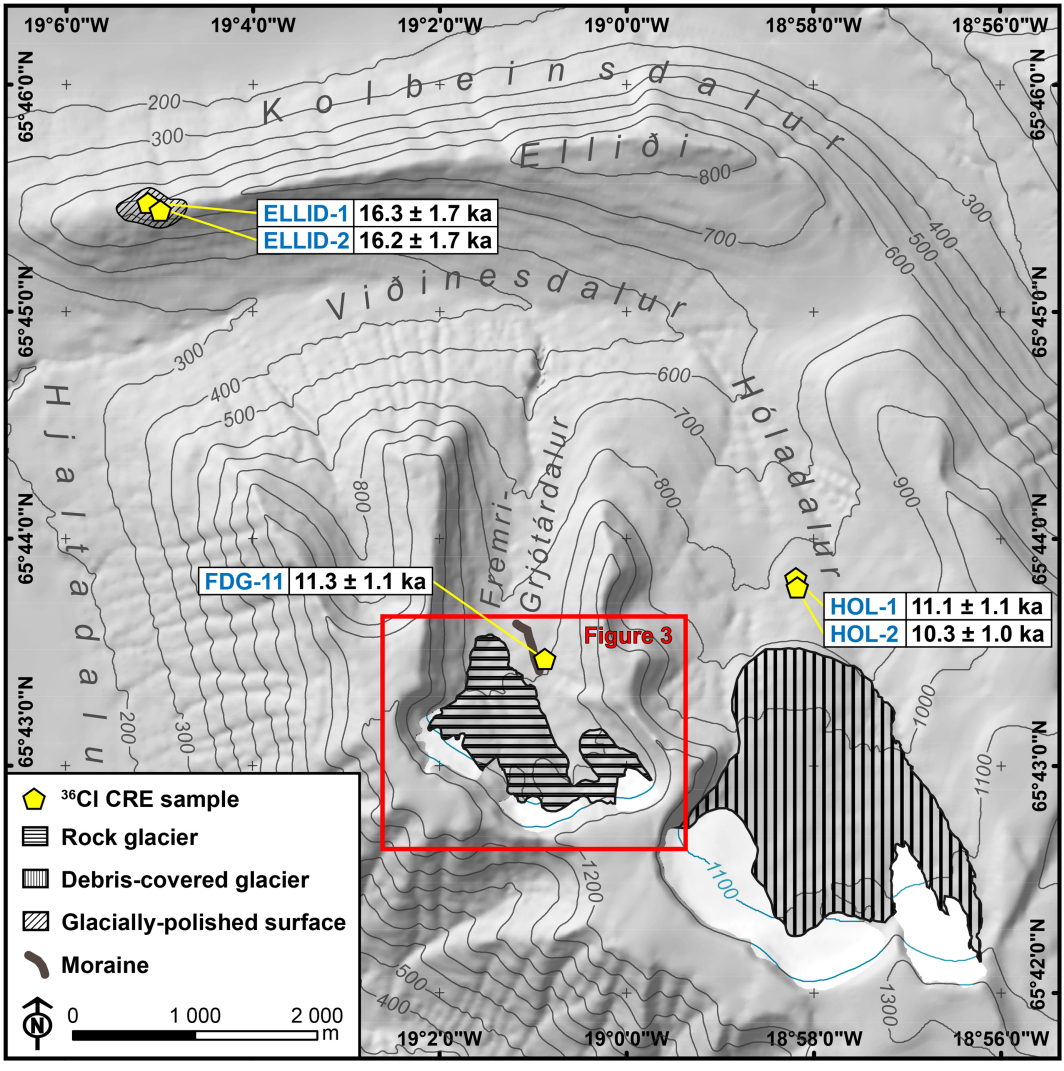
19°6'0"W
19°4'0"W
19°2'0"W
19°0'0"W
18°58'0"W
18°56'0"W
65°46'0"N
65°45'0"N
65°44'0"N
65°43'0"N
65°42'0"N
Kolbeinsdalur
Elliði
Viðinesdalur
Hjaltadalur
Hóladalur
Eremri-Grjótárdalur
ELLID-1 16.3 ± 1.7 ka
ELLID-2 16.2 ± 1.7 ka
FDG-11 11.3 ± 1.1 ka
HOL-1 11.1 ± 1.1 ka
HOL-2 10.3 ± 1.0 ka
Figure 3
36Cl CRE sample
Rock glacier
Debris-covered glacier
Glacially-polished surface
Moraine
0
1 000
2 000
m

Figure 6

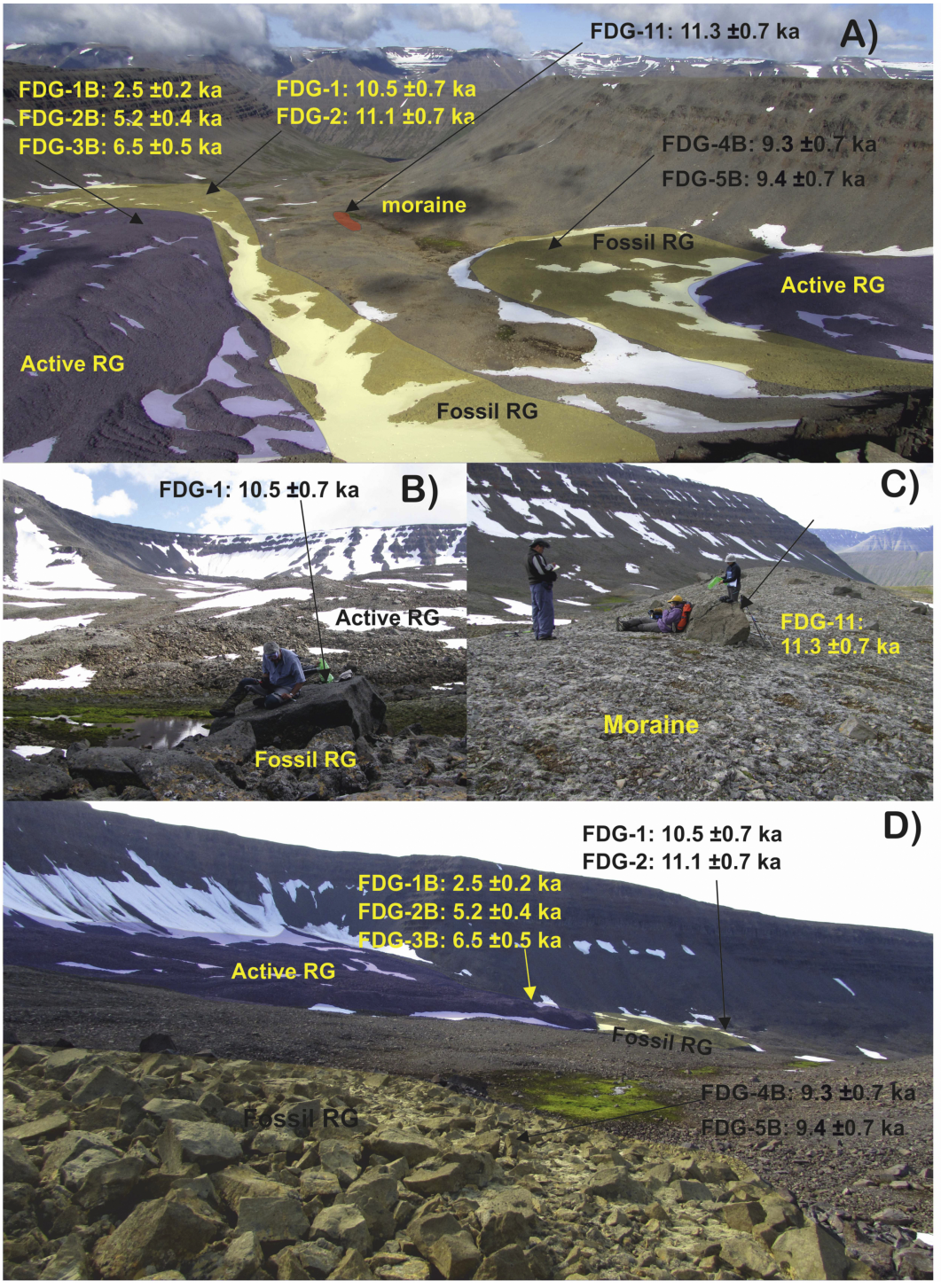
A)
FDG-11: 11.3 ±0.7 ka
FDG-1B: 2.5 ±0.2 ka
FDG-2B: 5.2 ±0.4 ka
FDG-3B: 6.5 ±0.5 ka
FDG-1: 10.5 ±0.7 ka
FDG-2: 11.1 ±0.7 ka
FDG-4B: 9.3 ±0.7 ka
FDG-5B: 9.4 ±0.7 ka
moraine
Fossil RG
Active RG
Active RG
Fossil RG
B)
FDG-1: 10.5 ±0.7 ka
Active RG
Fossil RG
C)
FDG-11:
11.3 ±0.7 ka
Moraine
D)
FDG-1: 10.5 ±0.7 ka
FDG-2: 11.1 ±0.7 ka
FDG-1B: 2.5 ±0.2 ka
FDG-2B: 5.2 ±0.4 ka
FDG-3B: 6.5 ±0.5 ka
Active RG
Fossil RG
FDG-4B: 9.3 ±0.7 ka
FDG-5B: 9.4 ±0.7 ka
Fossil RG

Figure 7

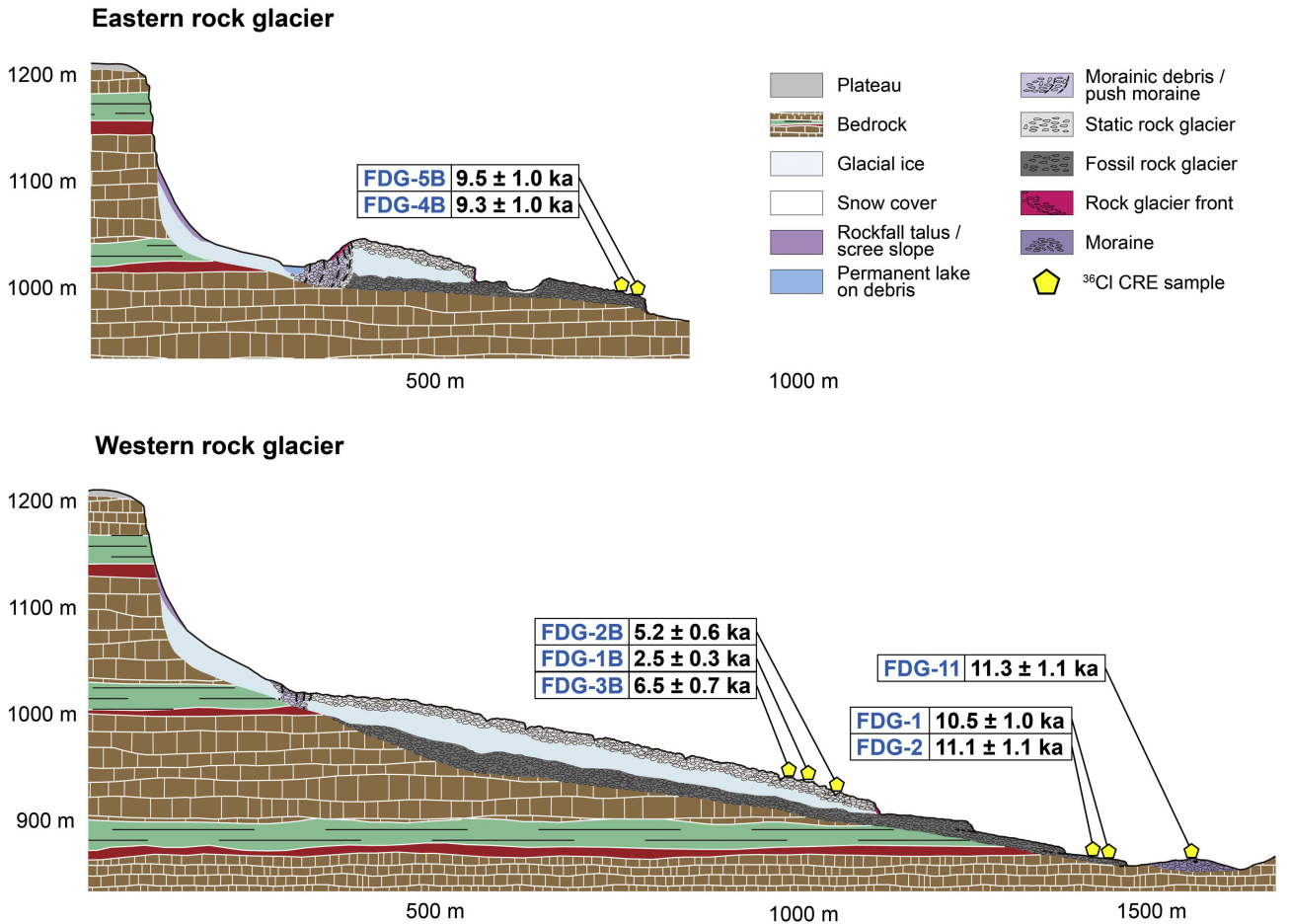
Fremri-Grjótárdalur rock glacier complex
Eastern rock glacier
1200 m
1100 m
1000 m
FDG-5B 9.5 ± 1.0 ka
FDG-4B 9.3 ± 1.0 ka
500 m
1000 m
Plateau
Bedrock
Glacial ice
Snow cover
Rockfall talus / scree slope
Permanent lake on debris
Morainic debris / push moraine
Static rock glacier
Fossil rock glacier
Rock glacier front
Moraine
36Cl CRE sample
Western rock glacier
1200 m
1100 m
1000 m
900 m
FDG-2B 5.2 ± 0.6 ka
FDG-1B 2.5 ± 0.3 ka
FDG-3B 6.5 ± 0.7 ka
FDG-11 11.3 ± 1.1 ka
FDG-1 10.5 ± 1.0 ka
FDG-2 11.1 ± 1.1 ka
500 m
1000 m
1500 m

Figure 8

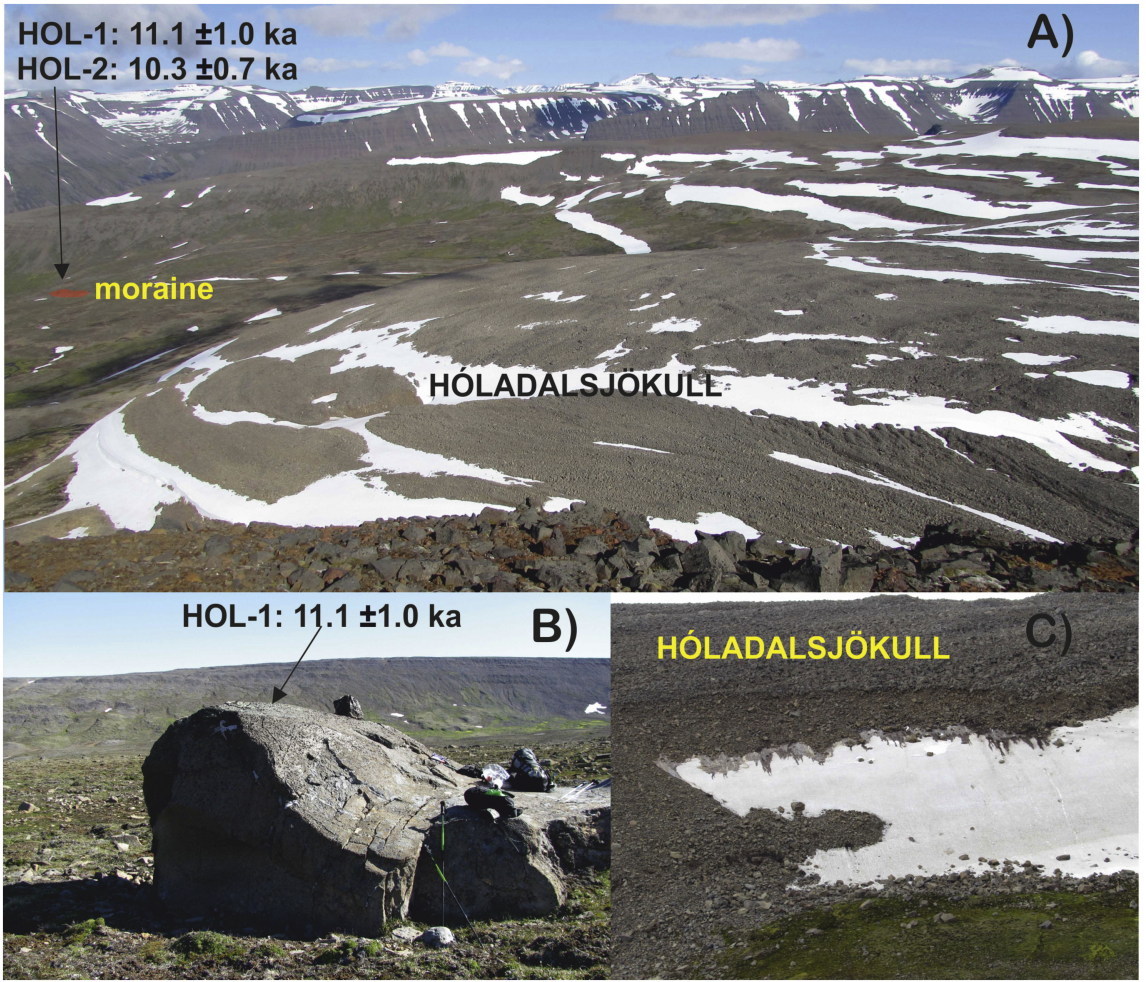
HOL-1: 11.1 ±1.0 ka
HOL-2: 10.3 ±0.7 ka
A)
moraine
HÓLADALSJÖKULL
HOL-1: 11.1 ±1.0 ka
B)
HÓLADALSJÖKULL
C)

Figure 9

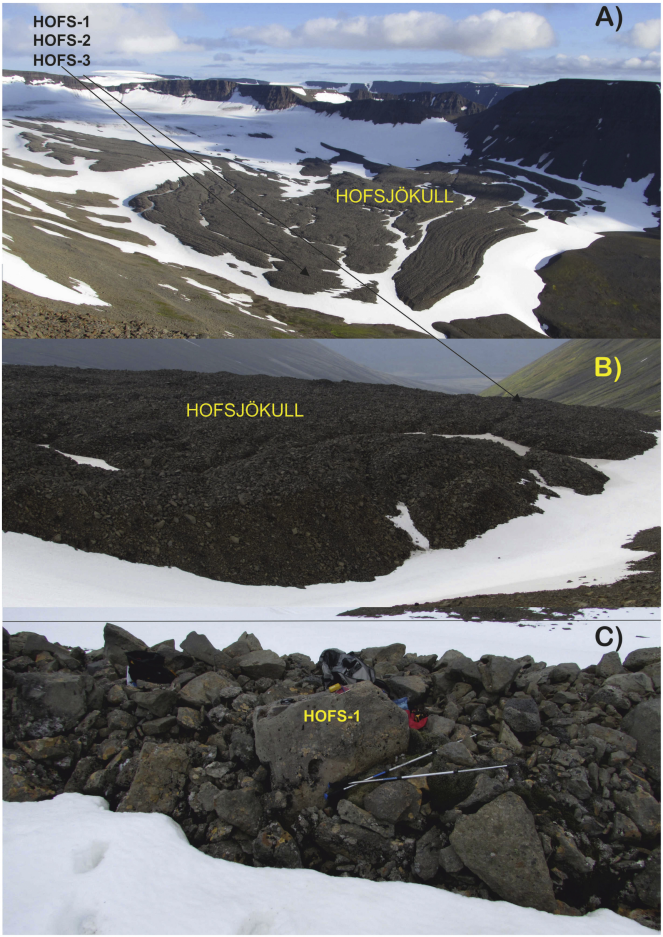

Figure 10

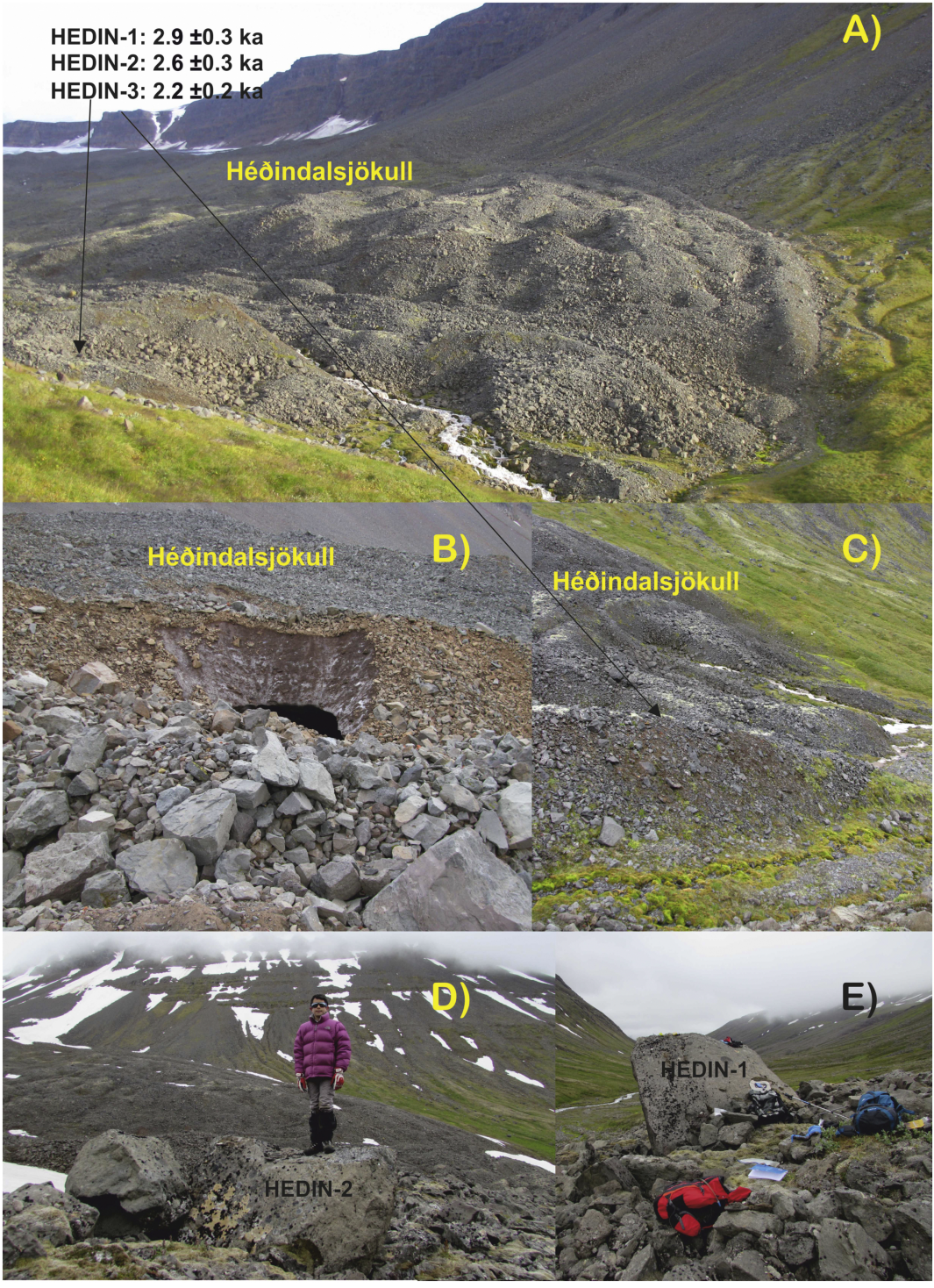
HEDIN-1: 2.9 ±0.3 ka
HEDIN-2: 2.6 ±0.3 ka
HEDIN-3: 2.2 ±0.2 ka
A)
Héðindalsjökull
B)
Héðindalsjökull
C)
Héðindalsjökull
D)
HEDIN-2
E)
HEDIN-1

Figure 11

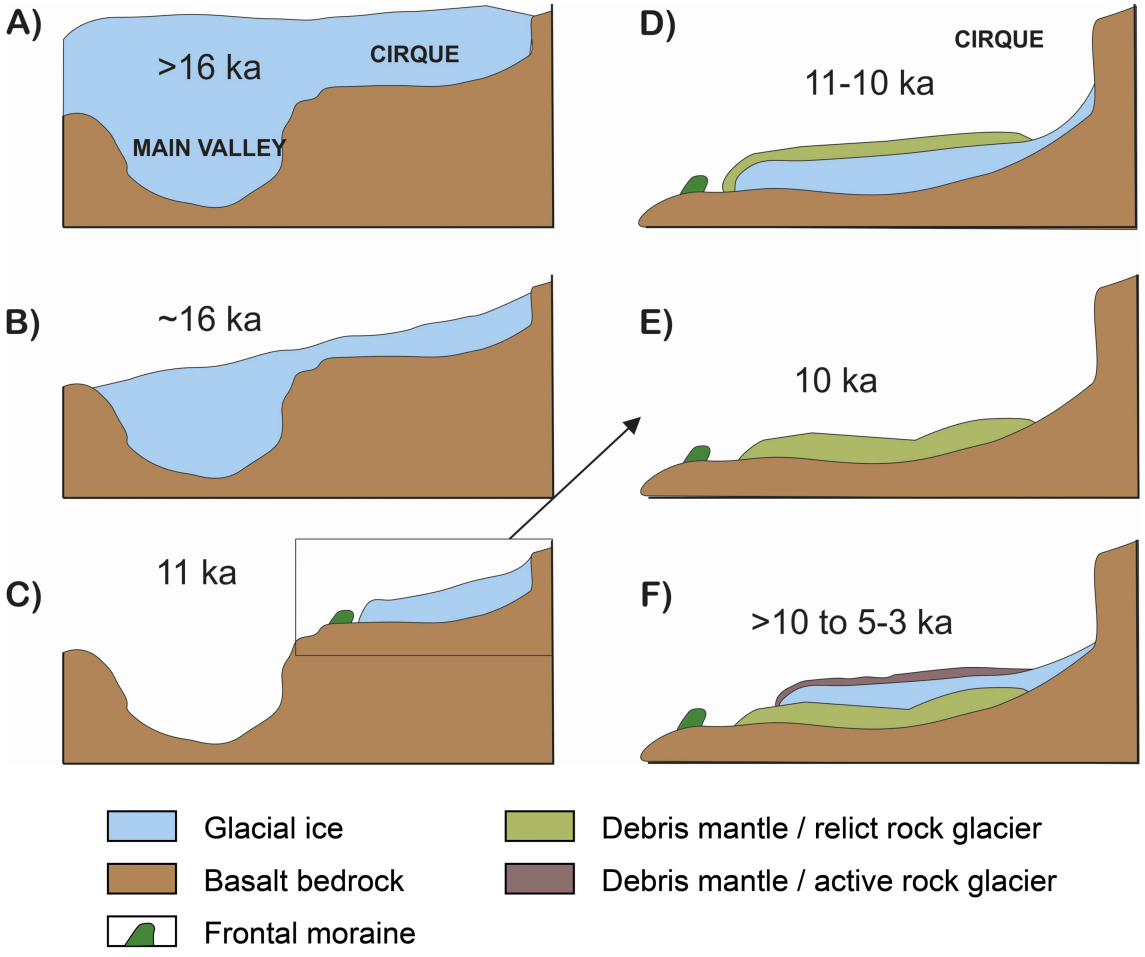
A)
>16 ka
CIRQUE
MAIN VALLEY
B)
~16 ka
C)
11 ka
D)
CIRQUE
11-10 ka
E)
10 ka
F)
>10 to 5-3 ka
Glacial ice
Basalt bedrock
Frontal moraine
Debris mantle / relict rock glacier
Debris mantle / active rock glacier

Figure 12